Universitá degli Studi di Padova

Dipartimento di Ingegneria Civile,
Edile ed Ambientale

Tesi di Laurea

Hydrologic regime and hydropower potential of the Bussento river (Italy)

Relatore: Prof. Gianluca BOTTER

Laureando: Michele CROSARA SELVATICO

Anno Accademico 2013-2014

Contents

Chapter 1

Introduction

Global policies on energy production hint at the reduction of carbon dioxide dispersed in the atmosphere. Many government programs and research studies highlight the negative role of CO_2 in the climatic changes occurred during last decades. In this context, renewable energies represent an important source for energy production. Recently, different techniques have been developed and/or more intensively exploited. Hydropower is probably the most ancient form of renewable energy and actually supplies about 15 % of the whole energy demand in the world. In Italy, for example, the energy demand is covered mainly by thermal power plant (71 %), while 15 % is associated to renewable plants (85 % of them are hydro plants). The development of hydro-electricity in the 20th century is typically associated with the construction of conventional plants that rely on large dams. Dams induce dramatic changes in the landscape (large areas are permanently inundated) and significant alterations of the downstream flow regime. Conventional hydropower plants are close to their saturation in most western countries, notwithstanding the huge environmental disturbance they induce on rivers and landscapes. During last decades a new type of hydroplants has become increasingly important: run-of-river plants. Instead of building large dams to accumulate water in an artificial reservoir, river flows are diverted and processed right ahead by a turbine allowing the release of diverted flows to the same river relatively close to the intake. These type of plants are suitable for the exploitation of a significant fraction of the residual hydropower potential of rivers, because of their relatively low construction costs and the lower environmental impact.

In Italy, the recent birth of the energy market has helped the spreading of renewable energy power plants because in the free market anyone can produce energy and sell it to the distribution network. In particular, the companies involved in the distribution are forced to supply a percentage of the whole expected demand from "green" producers at a fixed fare (renewable energy prices are high and guaranteed generally for 15 years). Hence governments incentive new investors to install green energy plants such as run-of-river micro-hydroplants by sustaining green energy prices through incentives. Particular attention has been devoted to promote this kind technology especially in less developed regions. Some studies have been carried out to assess the feasibility of hydroelectric plants in mountain territories of southern Italy, for the exploitation of the available residual hydropower potential. The research consists on the characterization of suitable sites for the installation of small hydropower plants, and the inquiries maked have revealed the presence of several sites theoretically exploitable. At any rate, between the characterization of potentially available hydroelectric resources and the evaluation of the economic profitability of a plant there must be a complete feasibility study and accurate costs analysis. In this regard, the characterization of the hydrologic regime plays an critical role. The amount of energy produced by a run-of-river hydropower plant, in fact, mainly depends on the sequence of streamflows workable by the plant during its lifetime, a feature which is controlled by the river flow availability. Streamflows observed a river cross section strongly fluctuate in time at multiple timescales, mirroring the variability of complex hydroclimatic processes, chiefly the rainfall forcing. The streamflow variability has been portrayed by hydrologists and engineers by means of the flow duration curve (FDC), or, alternatively, by the probability density function (PDF) of the streamflows. The shape of the duration curve places a substantial constraint on the optimal capacity (i.e. the maximum flow a plant can process) and other design attributes of a run-of-river plant.

Chapter 2

Characterization of the hydrologic regime

2.1 Streamflow regimes

The analytical classification of river flow regimes used in this thesis is grounded on a mechanistic analytical model that provides a stochastic description of daily streamflow dynamics. The latter are assumed to be the result of the superimposition of a sequence of flow pulses generated by flow producing rainfall events. These events are a subset of the overall rainfall, as they consist of the events bringing enough water to fill the soil-water deficit created by plant transpiration in the root zone.

Rainfall events are modeled as spatially uniform Poisson processes with exponentially distributed depths with mean α_P $[mm]$ and mean frequency λ_P $[d^{-1}]$. Being the flow-producing rainfall a subset of the overall rainfall, they are modeled as marked Poisson processes, with reduced mean frequency λ, which is always lower or equal to the mean frequency of rainfall. The ratio λ/λ_P expresses the ability of the the near surface soil moisture to filter the incoming rainfall forcing. For this reason, while the parameters α_P and λ_P are only a function of climate, λ depends also on soil properties and vegetation, in addition to climatic variables like temperature, humidity and wind speed. Mathematically using the crossing properties of soil moisture, it can be shown that:

$$\lambda = \eta \frac{exp(-\beta^{-1})\beta^{-\frac{\lambda_P}{\eta}}}{\gamma(\lambda_P/\eta, \beta^{-1})} \tag{2.1}$$

In equation (2.1), λ is function of the daily rainfall frequency and of climate/soil parameters, namely β (mean rainfall depth) and η (mean transpiration rate), both normalized to the depth of water available for plants in the root zone.

When the precipitation depth is large enough to determine the exceedance of the field capacity in the root zone, the excess is eliminated by the catchment hydrological response, quantified by the term k $[d^{-1}]$, function of catchment-scale morphological and hydrological attributes. The parameter k represents the inverse of the time scale of the idrograph and depends on pedological and morphological features. It can be estimated assuming that the root zone behaves like a linear reservoir, where each pulse of water inflow produces an instantaneous increase of discharge in the river followed by an exponential decrease with rate parameter k. The equations governing the behavior of a reservoir are:

$$Q = kV, \tag{2.2}$$

where V is the volume of water stored in subsurface environment, and

$$p - Q = \frac{dV}{dt}. \tag{2.3}$$

Considering instantaneous pulses forced by rain, it can be imposed $p = 0$, hence equations (2.2) and (2.3) can be written as:

$$\frac{dQ}{dt} = -kQ \tag{2.4}$$

Whose solution is:

$$Q(t) = Q_0 exp[-kt]. \tag{2.5}$$

Hence, the value of the recession rate k can be calculated as the mean of all the k values obtained for each event, by a liner regression of the temporal derivative dQ/dt compared to the corresponding discharge Q.

According to the assumptions made, the flow-producing rainfall events can be described as a marked Poisson process similar to the overall rainfall. These events

are assumed to have exponentially distributed depths, instantaneous durations and mean interarrival equal to $1/\lambda$. Since streamflow dynamics reflect rainfall events, the idrograph experiences positive jumps, exponentially distributed with mean $k\alpha$, and exponential decays.
The PDF of the normalized streamflow is obtained by the solution of the master equation:

$$\frac{\partial p(Q,t)}{\partial t} = \frac{\partial [kQp(Q,t)]}{\partial Q} - \lambda p(Q,t) + \frac{\lambda}{\alpha k}\int_0^Q p(Q-z,t)exp[-z/(\alpha k)]dz. \quad (2.6)$$

The steady state solution of equation (2.6) is a gamma PDF with mean

$$\mu = \lambda\alpha, \quad (2.7)$$

variance,

$$Var = \lambda k\alpha^2, \quad (2.8)$$

coefficient of variation

$$CV = \sqrt{k/\lambda} \quad (2.9)$$

shape parameter

$$s = \lambda/k \quad (2.10)$$

and rate parameter

$$r = \alpha k \quad (2.11)$$

River flow regimes can be classified as persistent or erratic on the basis of the ratio λ/k.
When flow-producing rainfall are frequent enough so that their mean interarrivals are smaller than the mean duration of the flow pulses ($\lambda > k$), the range of streamflows observed between two subsequent events is reduced and a persistent supply of water is guaranteed to the river from catchment soil. The ratio λ/k is greater than 1 and the flow regime is defined as persistent, resulting in river

flows weakly variable around the mean, and hence more predictable. This kind of regimes are typically observed during humid, cold seasons in slow responding catchments.

For persistent regimes:

- $\lambda/k > 1$
- Coefficient of Variation: $CV < 1$
- Shape parameter: $s > 1$

If the mean interarrival between flow producing rainfall events is larger than the mean duration of flow pulses ($\lambda < k$), the range of streamflows observed between two subsequent rainfall events is large because the river has enough time to dry significantly before the arrival of the next pulse. The ratio λ/k is lower than 1 and the result is a flow regime characterized by low discharges with high variance. This kind of regime is defined erratic and it is typical of fast responding catchments during season with sporadic rainfall events or during hot humid seasons.

For erratic regimes:

- $\lambda/k < 1$
- Coefficient of Variation: $CV > 1$
- Shape parameter: $s < 1$

2.2 PDF parameter estimation: general methodology

The main parameters used by the model for the streamflow distribution are:

- the main depth of rainfall events α_P;
- the recession time constant k;
- the frequency of flow producing events λ.

The mean depth of rainfall events has been computed from rainfall records as the observed mean daily depth during wet days.

The recession rate has been derived through a linear regression between the estimated temporal derivative of Q (dQ/dt) and the corrisponding observed discharges, expressed as the mean value of discharges in the interval dQ. To exclude the effect of fast flows, which have a limited impact on the flow distribution but

may significantly constrain the regression, only the discharges falling within the 0.9 quantile of the distribution have been considered.
The mean frequency of flow producing events can be expressed by the equation (2.1)as a function of the frequency λ_P and of some soil, vegetation and climate parameters. Taking on account that landscape information are not alwais available and, to make the estimation of λ easier, precipitation data and streamflow data have been combined, and the mean frequency of flow producing rainfall has been estimated as:

$$\lambda = \frac{\langle Q \rangle}{\alpha_P}, \tag{2.12}$$

where:

$$\langle Q \rangle = \frac{1}{\Delta T} \int_0^{\Delta T} Q(t)\, dt \tag{2.13}$$

where ΔT represents a reference time period.
Equation (2.12) is obtained equaling the observed mean specific discharge $\langle Q \rangle$ and the analytical mean of Q according to the stochastic model. The long term water balance, according to the stochastic odel, can be written as:

$$\langle P \rangle = \langle Q \rangle + \langle ET \rangle \tag{2.14}$$

where $\langle ET \rangle$ is the mean evapotranspiration in the reference time period. Equation (2.14) can be expressed as:

$$\lambda_p \alpha_P = \lambda \alpha_P + \langle ET \rangle \tag{2.15}$$

2.3 Baseflows and flow regime

In this thesis, the baseflow is defined as the portion of the streamflow which has no causal relationship with flow generating rainfall events. The presence of baseflow can be due to several reasons, like e.g. melting of snow during spring, deep subsurface flow or delayed shallow subsurface flow (carryover across seasons), contribution of water originating from surfaces that are located outside the catchment itself.

A general equation for the mean specific baseflow during the season i can be written as:

$$\langle Q_B \rangle_i = \langle Q_{Bin} \rangle_i + \langle Q_{Bout} \rangle_i \tag{2.16}$$

where $\langle Q_{Bin} \rangle_i$ is a mean specific baseflow discharge coming from inside the catchment, whose presence has to be justified with a water balance done in the whole river basin, while $\langle Q_{Bout} \rangle_i$ is the mean specific baseflow discharge coming from a source located outside of the catchment.

The main problem during the PDF parameters estimation correlated to the presence of baseflows concerns the evaluation of the parameter λ with the equation (2.12). In fact, in this case, the observed mean specific discharge $\langle Q \rangle_i$ is:

$$\langle Q \rangle_i = \langle Q_H \rangle_i + \langle Q_B \rangle_i \tag{2.17}$$

where $\langle Q_H \rangle_i$ is the discharge associated to rainfall inputs taking place during the season i and $\langle Q_B \rangle_i$ is the mean specific baseflow. The former is actually due to the hydrologic response of the catchment to flow producing events, while the latter is not.

Hence, the value of λ obtained through the equation (2.12) is over-estimated.

It is thus important, to get physycally meaningful parameters, to assess the presence of baseflow and properly account for it in the procedure of parameter estimation.

Usually the available data series are daily discharges and daily rainfall depths. Thanks to the available data it is possible, calculating the observed seasonal runoff coefficients, to understand the significance of baseflows contribution to the total discharge. The catchment's runoff coefficient C_R, referred to a given time period, is calculated as:

$$C_R = \frac{V_R}{V_P} \tag{2.18}$$

where V_R $[m^3]$ represents the volume of water flown through the closure section during the period ΔT, calculated as:

$$V_R = \int_0^{\Delta T} Q(t)\, dt \tag{2.19}$$

and V_P $[m^3]$ is the volume of rainfall precipitated in the catchment during the period ΔT. The latter is calculated using an averaged rainfall depth $\overline{h}$:

$$V_P = \int_0^{\Delta T} \overline{h}(t)\, dt \tag{2.20}$$

If $C_R > 1$, this means that discharges are not due only to precipitations, but there is a notable presence of a baseflow. For example, in spring C_R of mountain catchments is generally higher than one, because of the melting of snow fallen in the previous winter and the consequent raising of the total discharge.

The presence of a baseflow can be noticed directly calculating the value of λ and comparing it with the value of λ_P. Three cases are possible:

- $\lambda < \lambda_P$ The mean frequency of flow producing events is lower than the mean frequency of events. This is the condition that reflects most of the systems. In this case the surface soil moisture filter the incoming rainfall forcing, which can't always generate flows. This filtering is mainly due to evapotranspiration (cfr. equation (2.1)).
- $\lambda = \lambda_P$ In this situation there is no filtering done by the soil and to every rainfall event corresponds the generation of a flow. This situation can take place only in presence of two particular conditions. The first is that soil moisture has to be maximum, otherwise part of the precipitation goes up to fill the moisture gap, decreasing the mean frequency λ. The second condition is that evapotranspiration must be null, in order to prevent the formation of the soil water deficit. This can happen, for example in case of cold and wet periods, when evapotranspiration can be considered null.
- $\lambda > \lambda_P$ The meaning of this condition is that the events generating flow are more common than rainfall events.

  This situation reveals the presence of baseflows. This condition could also be determined by the presence of errors in the rainfall measurements, leading to an underestimation of the parameter λ_P. However in case of wrong data an hydrologic analysis based on this method would be definitely impossible.

Another useful tool to get initial deductions and first information about the hydrologic regime is the possibility to select a year of observations, which can be taken as a reference for initial guesses.

In case of a long period of observation, it can be built an *"average year"*, in which the succession of the flow is obtained by calculating the average during corresponding time intervals. So the average year will be formed, for example, by 12 values representing the average of the monthly mean discharges. The *"average year"* is a theoretical object and it describes nothing than the average hydrological character of the watercourse. And such it is not so useful for the purpouse of this thesis.
Instead, it is much more useful to consider the *"typical year"*, defined determining the deviations between measures of each annual sequence and the average year. For example, adopting average monthly discharges, deviations σ_i from the corresponding average monthly values are calculated for each month of the year under review. So the *"typical year"* is the year for which the condition:

$$\sum_{1}^{12} \sigma_i^2 = min \tag{2.21}$$

is satisfied.

2.4 Characterization of the hydrologic regime in presence of baseflow

The method is based on the separation of the stremflow into two components, as expressed by equation (2.17), assuming that the existence of the baseflow is due to the presence of discharges which are not the hypodermic response to flow producing rainfall events.
In order to take into account the possibility that a part of the incoming rainfall could leave the catchment as baseflow, through slow response, it is assumed that the incoming rainfall is first filtered by soil moisture dynamics and then splitted into two independent Poisson processes:

- the generation of hypodermic flow;
- the generation of baseflow.

Accordingly, a new parameter must be introduced, that represents the mean frequency of baseflow producing events, λ_S.
Using this framework, in case of baseflow, the water balance equation can be written, for the season i, as:

$$\langle P \rangle_i = \langle Q_H \rangle_i + \langle Q_S \rangle_i + \langle ET \rangle_i \tag{2.22}$$

where:

- $\langle Q_H \rangle_i$ is given by:

$$\langle Q_H \rangle_i = \lambda_H \alpha_P \tag{2.23}$$

  where λ_H is the mean frequency of events generating hypodermic (fast) flows.
- $\langle Q_S \rangle_i$, represent the mean specific discharge which constitutes the slow runoff response, given by:

$$\langle Q_S \rangle_i = \lambda_S \alpha_P \tag{2.24}$$

Equation (2.22) can be written also as:

$$\lambda_P \alpha_P = \lambda_H \alpha_P + \lambda_S \alpha_P + \langle ET \rangle_i \tag{2.25}$$

$$(\lambda_P - (\lambda_H + \lambda_S))\alpha_P = \langle ET \rangle_i \tag{2.26}$$

Formally, equation (2.26) is very similar to equation (2.15). Both express the flow-producing rainfall as a subset of the overall rainfall, modeling it as marked Poisson process, with a certain mean frequency. The difference is in separating the flow producing rainfall on the basis of the characteristics of the produced runoff, in this case, the hypodermic (fast) one and the slow one.
Introducing:

$$\lambda^* = \lambda_H + \lambda_S \tag{2.27}$$

It can be written that:

$$\lambda^* = \frac{\langle P \rangle_i - \langle ET \rangle_i}{\alpha_P} \tag{2.28}$$

So the value of λ^* can be obtained from (5.15) knowing rainfall features and $\langle ET \rangle_i$. On the other hand, the value of evapotranspiration can be calculated using the FAO approach:

$$\langle ET \rangle_i (s,t) = k_{Si} k_{Ci} \langle ET_O \rangle_i \tag{2.29}$$

where:

- k_{Si} is the mean seasonal water stress coefficient, which depends on the soil water content s with the relation:

$$k_S(s) = \begin{cases} 0 & \text{if } s < s_w \\ \frac{s-s_w}{s^*-s_w} & \text{if } s_w < s < s^* \\ 1 & \text{if } s > s^* \end{cases} \tag{2.30}$$

- k_{Ci} is the mean seasonal crop coefficient. This coefficient depends on time t: in fact plants transpiration varies during the year, following the life cycle of the plants;
- $\langle ET_O \rangle_i$ is the value of the seasonal mean specific potential evapotranspiration, which can be obtained with a good approximation using, for example, the Penman-Monteith equation.

Supposing that λ_H can be obtained from the analysis of the discharge timeseries, value of λ_S can be determined as:

$$\lambda_S = \lambda^* - \lambda_H \tag{2.31}$$

Values of λ_P and α_P, implicitely required to derive λ_S from equations (2.23) and (5.15), can be calculated using the method explained in section 2.2.

In this way, all the terms in equation (2.26), which gives the subdivision of the rainfall, are defined.

Ending, it is necessary to determine the link existing between $\langle Q_S \rangle_i$ and $\langle Q_B \rangle_i$. $\langle Q_S \rangle_i$ is defined as a slow runoff response, and, as said before, it will constitute the part of $\langle Q_B \rangle_i$ which comes from inside the basin, $\langle Q_{Bin} \rangle_i$. The dynamics followed by $\langle Q_S \rangle_i$ in becoming $\langle Q_{Bin} \rangle_i$ are unknown, but it can be assumed that, considering an appropriate time period T including n seasons, the whole volume of slow runoff water is discharged as baseflow. Under this hypothesis it can be written that:

$$\left(\sum_{i=1}^{n} \langle Q_S \rangle_i \right) \cong \left(\sum_{i=1}^{n} \langle Q_{Bin} \rangle_i \right) \tag{2.32}$$

Formally, the seasonal internal baseflow $\langle Q_{Bin} \rangle_i$ must be formally subdivided into two parts. In fact, it can be constituted of a certain discharge part coming from

the previous season (*carryover discharge*), which will be called $\langle Q_{Bco} \rangle_{i-1}$ and of a part due to the slow runoff of the season itself $\langle Q_S \rangle_i$. A given fraction of $\langle Q_S \rangle_i$ in turn, a part of it will constitute a carryover for the subsequent seasons. This is shown by the relation (5.5):

$$\langle Q_{Bin} \rangle_i = \left(\langle Q_{Bco} \rangle_{i-1} + \langle Q_S \rangle_i \right) - \langle Q_{Bco} \rangle_i \tag{2.33}$$

It is important to point out that it is not possible to identify which part of $\left(\langle Q_{Bco} \rangle_{i-1} + \langle Q_S \rangle_i \right)$ actually becomes $\langle Q_{Bin} \rangle_i$ because of the unknown contribution of $\langle Q_{Bco} \rangle_i$.

The method admits the existence of a contribution of an external source equal to the mean specific discharge $\langle Q_{Bout} \rangle$ if necessary to balance water specific discharges in period ΔT. $\langle Q_{Bout} \rangle$ is assumed to be constant across the different seasons.

Thus, the external contribution takes place if:

$$\left(\sum_{i=1}^{n} \langle Q_B \rangle_i \right) > \left(\sum_{i=1}^{n} \langle Q_{Bin} \rangle_i \right) = \left(\sum_{i=1}^{n} \langle Q_S \rangle_i \right) \tag{2.34}$$

Meanwhile, the contribution from external sources for each season i is calculated as:

$$\langle Q_{Bout} \rangle = \frac{1}{n} \left(\sum_{i=1}^{n} \langle Q_B \rangle_i - \sum_{i=1}^{n} \langle Q_S \rangle_i \right) \tag{2.35}$$

2.5 Estimating the parameters of the streamflow distribution in presence of baseflow

The PDF's parameters estimation method described in section 2.2 has to be modified to account for the baseflow. In particular, the mean total discharge $\langle Q \rangle_i$ is subdivided into two parts, $\langle Q_H \rangle_i$ and $\langle Q_B \rangle_i$. Under the assumption that Q_{Hi} and Q_{Bi} are indipendent random variables, the PDF of the overall specific discharge Q during a given season i can be expressed as:

$$p_i(Q) = p_{Hi}(Q_H) * p_{Bi}(Q_B) \tag{2.36}$$

According to equation (2.36) the probability density function of Q is calculated as the *convolution* of the probability density functions of the baseflow and the hypodermic discharge.
These two PDF are defined by two different sets of parameters, obtained with two different methods, as discussed below.

2.5.1 Parameters estimation for the hypodermic discharge

Concerning the hypodermic discharge the parameters that need to be estimated are λ_H, k and α_P.
The frequency of λ_H can be obtained thanks to equation (2.23) suitably modified:

$$\lambda_H = \frac{\langle Q_H \rangle_i}{\alpha_P} = \frac{(\langle Q \rangle_i - \langle Q_B \rangle_i)}{\alpha_P} \tag{2.37}$$

λ_H is thus obtained from discharge data. However, the calculation of the mean value of the baseflow discharge is the main problem, because there are no criteria for understanding how to split these flows.
Hence, it is necessary to find another way for the determination of the parameter λ_H.
If discharge data series are available, looking to their plot, it can be seen a certain number of flow peaks, which reflects the number of times in which soil moisture gap has been filled by rainfall, leading to the generation of the hypodermic flow. In other words, λ_H represents the frequency of rainfall events generating hypodermic flow. This means that the value of mean frequency of hypodermic flow producing rainfall events in time period ΔT can be obtained as:

$$\lambda_H = \frac{N_E}{\Delta T} \tag{2.38}$$

where N_E is the number of flow producing rainfall events.
This value of λ_H is approximated, because of the uncertainty in recognising the peaks, though it represents a good measure of the mean frequency.
Once obtained a value for λ_H, it is possible to calculate the mean baseflow for the same period as:

$$\langle Q_B \rangle_i = \langle Q \rangle_i - \lambda_H \alpha_P. \tag{2.39}$$

The value of λ_H, calculated in this way, fullfills the condition $\lambda_H < \lambda_P$.
The recession time constant k for the hypodermic discharge can be calculated by assuming that the dynamics of Q during a given season are mostly related to the variability of Q_H:

$$\frac{dQ_H/dt}{Q_H} = \frac{dQ/dt}{Q} = -k \tag{2.40}$$

Equation (2.40) enables the calculation of k using the available data of discharge Q.
The mean depth of rainfall events α_P has been computed from rainfall records as the observed mean daily depth during wet days, as discussed in section 2.2.
The PDF of the hypodermic flow, $p_H(Q_H)$, is thus defined as:

$$p_H(Q_H) = \frac{(s_H)^{{r_H}^{-1}}}{\Gamma({r_H}^{-1})} Q_H^{s_H-1} e^{-Q_H {r_H}^{-1}} \tag{2.41}$$

where the shape parameter s_H is calculated as:

$$s_H = \lambda_H / k \tag{2.42}$$

and the rate parameter r_H is:

$$r_H = \alpha_P k \tag{2.43}$$

2.5.2 Parameters estimation for the baseflow

The PDF of baseflow is assumed be a gamma distribution. The parameters defining the PDF of the baseflow discharge are calculated using a different approach, based on two main assumptions:

- the mean specific value $\langle Q_B \rangle_i$, estimated from equation (2.39) corresponds to the mean analitical value of the PDF of Q_B;
- the coefficient of variation of the seasonal baseflow is correlated to the mean specific rainfall with the relation:

$$CV(\langle Q_B \rangle) = CV(\langle P \rangle) \tag{2.44}$$

Based on the mean value and the variance of a $\langle Q_B \rangle$, under these assumptions, it is possible to get the parameters of the corresponding baseflow PDF (see equations (2.7), (2.8), (2.10) and (2.11)).

The mean specific rainfall has shown a good correlation with the specific baseflow. Different catchments show different behaviors in releasing water through slow processes, depending mainly on climate and morphological features of the basin. Therefore, the correlation between rainfall and baseflow in different seasons is something that needs to be properly assessed.

Starting from daily rainfall and discharge data series, the values of the seasonal mean specific rainfall and baseflows discharges can be calculated for each year of observation. Generally, the mean baseflow of a given season is well correlated with the rainfall observed during the previous season and/or the season under consideration.

Based on available data, in this work we assumed a linear correlation between $\langle Q_B \rangle_i$ and $\langle P \rangle_{i,i-1}$, the average specific rainfall during the season i and $i-1$ (the season at hand and the previous one):

$$CV(\langle Q_B \rangle_i) = CV(\langle P \rangle_{i,i-1}) \tag{2.45}$$

The shape and rate parameters of the baseflow PDF can thus be obtained from the mean baseflow $\langle Q_B \rangle_i$ and its variance $var(\langle Q_B \rangle_i) = CV(\langle Q_B \rangle_i) \langle Q_B \rangle_i^2$:

$$s_B = \frac{\langle Q_B \rangle_i^2}{var(\langle Q_B \rangle_i)} \tag{2.46}$$

$$r_B = \frac{var(\langle Q_B \rangle_i)}{\langle Q_B \rangle_i} \tag{2.47}$$

The baseflow discharge gamma PDF $p_B(Q_B)$ is thus defined:

$$p_B(Q_B) = \frac{(s_B)^{{r_B}^{-1}}}{\Gamma({r_B}^{-1})} Q_B^{s_B - 1} e^{-Q_B {r_B}^{-1}} \tag{2.48}$$

Equation (2.36) is thus defined, and the PDF of the discharge Q, can be obtained.

Chapter 3

Evaluation of the hydropower potential

3.1 Optimization of the energy production in a run-of-river plant

The energy produced by a hydropower plant depends mainly on three variables.

- the net hydraulic head, calculated as the difference between the gross hydraulic head and the energy losses within the plant;
- the workable flow (q_w), that also impacts the turbine efficiency;
- the turbine efficiency, which mainly depends on the turbine type and on the ratio $x = q_w/q_D$.

The following mathematical derivation will be focused on a plant equipped with a single turbine, where the hydropower plant capacity (the maximum flow that can be processed) is taken as the only decision variable, thereby assuming the remaining design attributes of the plant to be known or derivable on the basis of the capacity.

The energy produced by a hydropower plant during a time period ΔT is the time integral of the time dependent power generated during ΔT:

$$E(q_D) = \rho g \, \eta_P \int_0^{\Delta T} H(t) \, \eta \left(\frac{q_w(t)}{q_D} \right) q_w(t) \, dt \tag{3.1}$$

where q_D is the plant capacity (i.e., design flow), ρ is the water density, g is the standard gravity, η_P is the efficiency of the plant, η is the turbine efficiency and H is the net hydraulic head. In the forthcoming calculations the head H is assumed to be a constant. Hence both the head losses and possible reductions of the gross head for incoming flows larger than q_D will be neglected.

In this context, the amount of energy produced by a run-of-river hydropower plant mainly depends on the sequence of streamflows workable by the plant during its lifetime, which is controlled by the river flow availability. The streamflow variability is portrayed by means of the probability density function $p(x)$ by which the flow duration curve of the streamflows, (FDC), defined as:

$$D(x) = FDC(x) = 1 - \int_0^x p(q)\, dq \tag{3.2}$$

can be obtained. In (3.2) the term $\int_0^q p(x)\, dx$ represents the not-exceedance probability of the discharge q.

The shape of the duration curve places a substantial constraint on the optimal capacity (i.e., the maximum flow a plant can process) and other design attributes of a run-of-river plant.

For time periods ΔT much longer than the correlation scale of the streamflows (e.g. few years, a decade, the lifetime of the plant), the incoming streamflows can be assumed to be ergodic, and the frequencies characterizing the different values of q_w in equation (3.1) are described by the probability density function of the workable flows, p_w. Therefore, the time integral of equation (3.1) can be replaced by a weighted integral over q_w, the weighting factor being p_w:

$$E(q_D) = \Delta T\, H\, \rho g\, \eta_P \int_0^\infty \eta \left(\frac{q_w}{q_D} \right) p_w(q_w)\, q_w\, dq_w \tag{3.3}$$

To further specify equation (3.3) and express the PDF of the flows processed by the plant, $p_w(q_w)$, in terms of the PDF of the incoming streamflows $p(q)$, the operation rules of a run-of-river power plant must be considered (Figure 3.1).

Due to flow requirements downstream of the intake, the flow which can be diverted from a river to the plant is the difference between the incoming streamflow q and the MFD (when such difference is positive). Moreover, the actual range of streamflows processed by the plant depends on the technical constraints of the turbine, namely

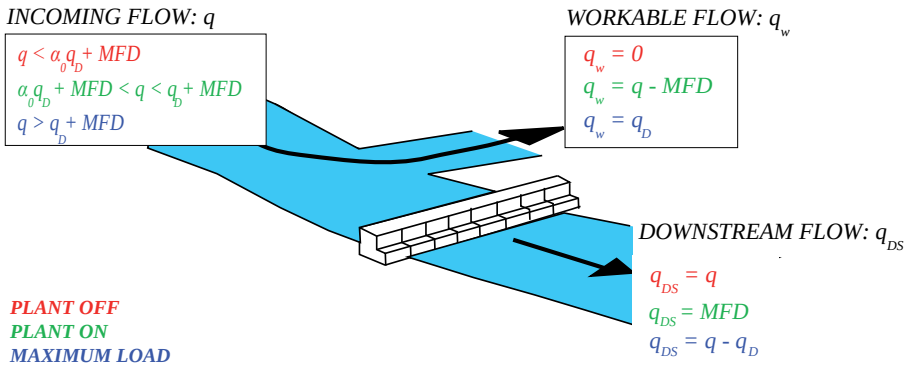

Figure 3.1: Scheme of functioning of a run-of-river hydropower plant with the derivation to the plant which respect the prescription of Minimum Flow Discharge in the river.

its capacity q_D, and the minimum workable flow q_C (i.e. cut-off flow), which is usually expressed as a fraction of q_D (i.e., $q_C = \alpha_0\, q_D$). In particular, when the flow which could be diverted $(q - MFD)$ is lower than the cut-off flow q_C, it cannot be processed and $q_w = 0$. This happens with probability $1 - D(q_C + MFD)$, $D(\cdot)$ being the duration curve of the inflows (i.e., $D(z) = \int_z^\infty p(q)dq$), as shown by the following equations:

$$\begin{aligned}\int_0^{\alpha_0 Q} p_w(q_w)\, dq_w &= 1 - \int_{\alpha_0 Q}^{\infty} p(q_w + MFD)\, dq_w = \\ &= 1 - \int_{\alpha_0 Q + MFD}^{\infty} p(q)\, dq = \\ &= 1 - D(\alpha_0 Q + MFD) \end{aligned} \tag{3.4}$$

On the other hand, when the diverted flows are in between the cut-off flow and the capacity of the plant, they are entirely processed by the plant, and $q_w = q - MFD$. Finally, when the flow which could be diverted exceeds the capacity of the plant, only the flow q_D is actually taken from the river and processed. This happens with a probability equal to $D(q_D + MFD)$, as the following expression demonstrate:

$$\begin{aligned}\int_Q^{\infty} p_w(q_w)\, dq_w &= \int_{q_D}^{\infty} p(q_w + MFD)\, dq_w = \int_{q_D + MFD}^{\infty} p(q)\, dq = \\ &= D(q_D + MFD) \end{aligned} \tag{3.5}$$

The *PDF* of the flows which are processed by the plant hence corresponds to the incoming streamflow *PDF*, p, (dashed line in Figure 3.2) simply translated leftward by a value equal to the *MFD*, with the two tails of the original distribution becoming two atoms of probability associated to $q_w = 0$ and $q_w = q_D$. The probability distribution of the workable flows $p_w(q_w)$ can thus be expressed as:

$$p_w(q_w) = p(q_w + MFD) \quad \text{if} \quad \alpha_0 q_D < q_w < q_D \tag{3.6}$$

while for $q_w = 0$ and $q_w = q_D$ we have two atoms of probability respectively equal to $[1 - D(\alpha_0 q_D + MFD)]$ (eq. 3.4) and $[D(q_D + MFD)]$ (eq. 3.5).

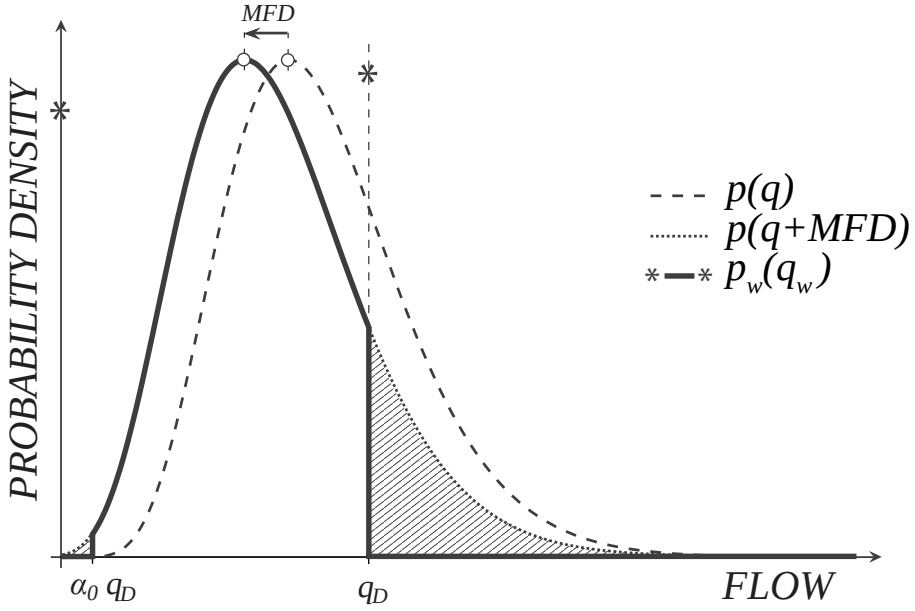

Figure 3.2: Probability distributions of streamflows ($p(q)$, dashed line), of river flows which can be diverted (dotted line) and of flows workable by an hydropower plant ($p_w(q_w)$, solid line and stars).

When the expression of the workable flow *PDF* given by equation (3.6) is used, equation (3.3) becomes:

$$\begin{aligned} E(q_D) \;=\; & \Delta T\, H\, \rho g\, \eta_P \left[\int_{\alpha_0 q_D}^{q_D} \eta\left(\frac{q_w}{q_D}\right)\, p(q_w + MFD)\, q_w\, dq_w + \right. \\ & \left. + \eta(1)\, q_D\, D(q_D + MFD) \right] \end{aligned} \tag{3.7}$$

The second term within the square brackets on the right hand side of equation (3.7) is originated from the atom of probability in correspondence of $q_w = q_D$, while the first term derives from the continuous part of the workable flow *PDF*. The maximization of the produced energy $E(q_D)$ requires to specify the efficiency function $\eta(x)$. The efficiency pertaining to each turbine type can be represented by means of specific curves characterized by distinctive shapes and working ranges. Examples of efficiency curves for different types of turbines are displayed with thick grey lines in Figure 3.3. The actual turbine efficiency curve will be approximated by a piecewise linear function.

When the turbine efficiency for different values of x is described by means of a piecewise linear function, its behavior can be described as follows: for x lower than α_0, the efficiency of the turbine is null; between α_0 and α_M, efficiency grows linearly from η_0 to η_M; for x larger than α_M, the efficiency is maximum η_M. The approximation can be formulated in analytical terms through the following expression:

$$\eta(x) = \begin{cases} 0 & \text{if } x < \alpha_0 \\ \frac{x-\alpha_0}{\alpha_M-\alpha_0}(\eta_M - \eta_0) + \eta_0 & \text{if } \alpha_0 \leq x < \alpha_M \\ \eta_M & \text{if } x \geq \alpha_M \end{cases} \tag{3.8}$$

which substituted into equation (3.7) yields:

$$\begin{aligned} E(q_D) \;=\; & \Delta T\, H\, \rho g\, \eta_P \left\{ \int_{\alpha_M q_D}^{q_D} \eta_M\, p(q_w + MFD)\, q_w\, dq_w + \right. \\ & + \eta_M\, q_D\, D(q_D + MFD) + \\ & \left. + \int_{\alpha_0 q_D}^{\alpha_M q_D} \left[\frac{q_w - \alpha_0 q_D}{\alpha_M q_D - \alpha_0 q_D}(\eta_M - \eta_0) + \eta_0 \right] p(q_w + MFD) q_w dq_w \right\} \end{aligned} \tag{3.9}$$

Once this analytical expression has been obtained, the value of q_D which gives the best result in terms of produced energy can be obtained. This can be done by computing the derivative dE/dq and setting it equal to zero. The value of q_D satisfying the equation $dE/dq = 0$ provides the optimal hydropower plant capacity. The first derivative of equation (3.9), is:

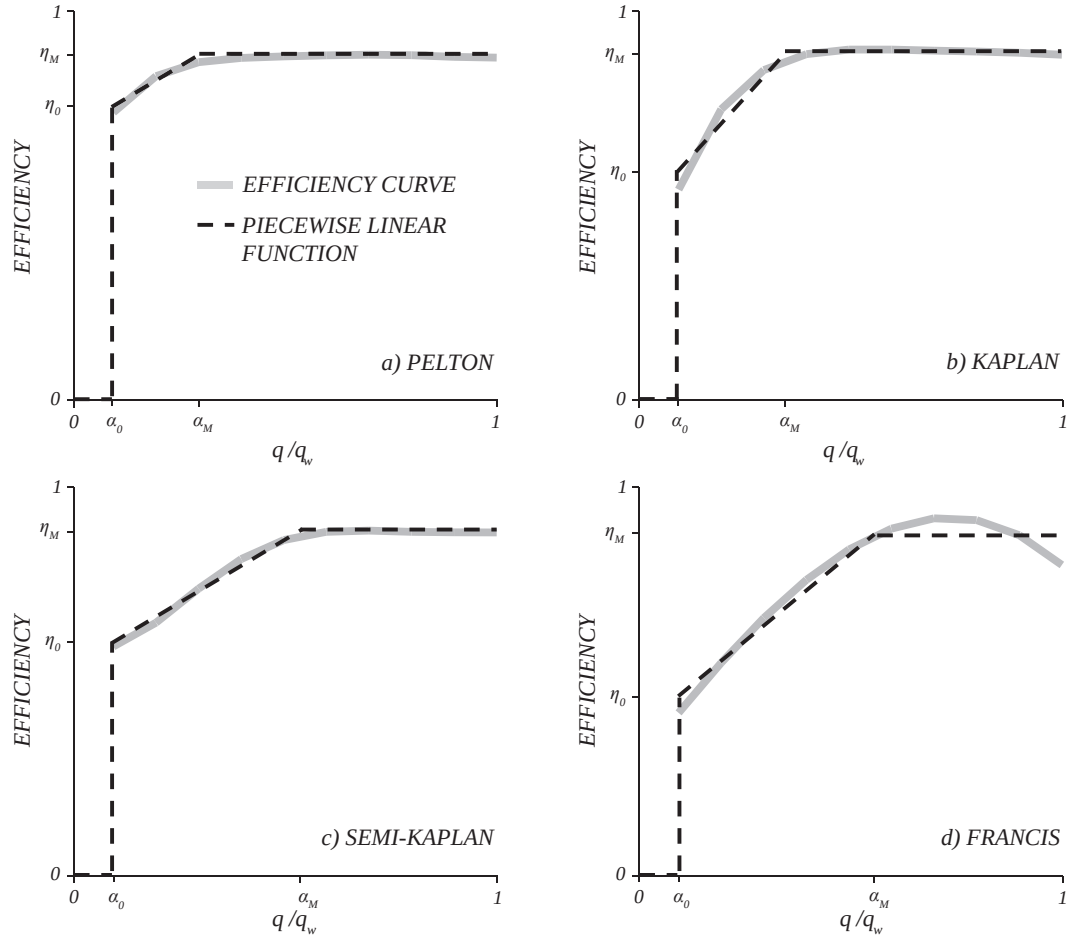

Figure 3.3: Efficiency curves for different turbine types (solid grey lines), taken from literature. The approximation given by the piecewise linear (dashed lines, equation (3.8)) functions is displayed for the different cases, with the validity boundaries of the different parts of these functions (α_0 and α_M) and the corresponding efficiency values (η_0 and η_M).

$$\frac{dE}{dq} = \Delta T\, H\, \rho g\, \eta_P \left[\eta_M\, D(q_D + MFD) + \eta_0\, \alpha_0\, q_D\, D'(\alpha_0 q_D + MFD) + \right. \\ \left. + \int_{\alpha_0}^{\alpha_M} \left(\frac{\eta_M - \eta_0}{\alpha_M - \alpha_0}\, x \right) q_D x\, D'(q_D x + MFD)\, dx \right] \tag{3.10}$$

The physical meaning of equation (3.10) can be evidenced by focusing on the terms within the square brackets. To this end the infinitesimal variation of the energy produced by an infinitesimal increment of the capacity is expressed as:

$$dE \propto \eta_M\, D(q_D + MFD)\, dq + \eta_0\, \alpha_0 q_D\, D'(\alpha_0 q_D + MFD)\, dq + \\ + \int_{\alpha_0}^{\alpha_M} \left(\frac{\eta_M - \eta_0}{\alpha_M - \alpha_0}\, x \right) q_D x\, D'(q_D x + MFD)\, dq\, dx \tag{3.11}$$

The first term at the right-hand side of equation (3.11) is the product between the percentage of time during which the design flow q_D is processed and the increment of the capacity, dq. Hence, this term represents the rise of processed volumes due to increased plant size. The second term (which is negative because $D'(z) = -p(z) < 0$) is the product between the value of the lower limit of the workable flows, $\alpha_0 q_D$, and the decrease of its duration, which is obtained computing the product between dq and the derivative of the duration curve evaluated in $\alpha_0 q_D + MFD$, $D'(\alpha_0 q_D + MFD)$. This second term thus represents the loss of processed volumes due to the increase of the minimum workable flow q_C. The third term, instead, represents the reduction of the energy produced in the range of the suboptimal efficiencies $\eta_0 < \eta < \eta_M$, induced by the change of duration associated to the various efficiencies. According to equation (3.11), an increase of q_D leads to an increase of E only if the energy obtained from the additional water volume processed exceeds the energy losses associated with the water volume the plant no longer works and the decrease of the energy produced in the range of suboptimal efficiencies. The condition providing the capacity which maximizes the produced energy, Q_{EN}, can be obtained by setting $dE/dq = 0$ in equation (3.10). Therefore, Q_{EN} satisfies:

$$D(q_D + MFD) = -\frac{\eta_0}{\eta_M} \alpha_0 q_D D'(\alpha_0 q_D + MFD) + \\ + \int_{\alpha_0}^{\alpha_M} \left(\frac{1 - \eta_0/\eta_M}{\alpha_M - \alpha_0} \right) q_D x^2 D'(q_D x + MFD) dx \tag{3.12}$$

Equation (3.12) provides some insight on the typical value of $D(Q_{EN})$. In most cases, the integral term of the above equation can be neglected, mainly because the integrand function is usually small and the range of integration is relatively narrow. Hence, equation (3.12) can be simplified as follows:

$$D(q_D + MFD) = \frac{\eta_0}{\eta_M}\alpha_0^2 q_D\, p(\alpha_0 q_D + MFD) \tag{3.13}$$

3.2 Optimization based on economic indexes

The actual optimization of run-of-river plants capacity is obviously based also on economic issues. Investors are indeed only interested in the earning they can get from hydropower plants and not in the energy produced by the plant. Due to the non linear increase of the costs with the size of the plant, the profits (calculated as the revenues minus the costs, mainly represented by initial costs to build the plant) are not proportional to the energy produced. The revenues generated by a run-of-river hydropower plant are calculated by multiplying the produced energy by the selling price of energy from renewable sources e_p, which is assumed here to be constant. To make a proper economic assessment of the hydropower project, we shall assume hereafter that the ergodicity hypothesis underlying equation (3.7) can be applied within each year of ΔT, so as the annual revenue $R_1(q_D)$ is the same every year. Hence, we can compute the annual proceeds $R_1(q_D)$ as:

$$R_1(q_D) = e_p\, E_1(q_D) \tag{3.14}$$

where $E_1(q_D)$ is $E(q_D)$ expressed by equation (3.9) with $\Delta T = 1$ year. The overall present value $R_n(q_D)$ of every cash inflow occurring during n years (e.g. the duration of state incentives or the lifetime of the plant, which are 15 in Italy for example) can be computed by means of the following expression:

$$R_n(q_D) = \sum_{k=1}^{n} \frac{1}{(1+r)^k}\, R_1(q_D) = \frac{1}{r}\left(1 - \frac{1}{(1+r)^n}\right) R_1(q_D) = \hat{r} R_1(q_D) \tag{3.15}$$

where r is the (constant) annual discount rate and $\hat{r} = \frac{1}{r}\left(1 - \frac{1}{(1+r)^n}\right)$ is an auxiliary variable expressing the multiplier used to compute the present value of the

overall cash inflows. Typically hydropower plants are characterized by initial investment costs much higher than the corresponding operation expenses. Therefore, the costs incurring during the functioning of the plant have been neglected to focus on the construction expenses. Several past studies have investigated the relation between construction costs and some key features of a hydropower plant, chiefly the nominal power and the hydraulic head, so, the construction costs are expressed as a function of the design flow (being all the other terms, like lenght of the adduction, being constants) as:

$$C(q_D) = a\, q_D^b \tag{3.16}$$

where a and b are empirical coefficients. Typical values for a and b can be derived from previous studies or via empirical estimates of the relationship between construction costs and plant features. While a can be highly variable from site to site, the parameter b has been found to be weakly variable around 0.6 in most cases.

In this work, some indexes to represent the profitability of an investment shall be introduced. One of the standard indexes is the Net Present Value (NPV) which is used to quantify the reliability of an investment. The Net Present Value of a sequence of cash inflows/outflows is defined as the sum of every cash flow discounted back to its present value. In this case all future cash flows are incoming flows (the proceeds obtained from the selling of the produced energy). Conversely, the only outflow is assumed to occur at time zero, and it is represented by the construction cost of the plant, evaluated here by assuming that the plant could be completed during the first year and neglecting possible financings and the related interests. Hence, the NPV can be computed as:

$$NPV(q_D) = R_n(q_D) - C(q_D) = \hat{r}\, R_1(q_D) - C(q_D) \tag{3.17}$$

The condition providing the capacity which maximizes the NPV, q_{NPV}, can be obtained by calculating $dNPV(q_D)/dq_D$ through equations (3.10), (3.14), (3.16) and (3.17), and setting it equal to zero. q_{NPV} hence should satisfy:

$$\begin{aligned} & \Big[\eta_M \, D(q_D + MFD) + \eta_0 \, \alpha_0 q_D \, D'(\alpha_0 q_D + MFD) \; + \\ + \int_{\alpha_0}^{\alpha_M} & \left(\frac{\eta_M - \eta_0}{\alpha_M - \alpha_0} \right) q_D x^2 \, D'(q_D x + MFD) \, dx \Big] \, \hat{r} \, e_p \, H \, \rho g \, \eta_P \;\; = \;\; a \, b \, q_D^{b-1} \end{aligned} \tag{3.18}$$

According to equation (3.18), the optimal design flow is achieved whenever the marginal revenues due to increased plant size are equal to the corresponding marginal cost.

Chapter 4

The Bussento catchment

4.1 The Bussento river, (Italy)

The Bussento river flows in the Salerno province (Campania), in southern Italy. Its contributing catchment is 316 km^2, and it is all included in the territory of the Cilento and Vallo di Diano national park.

The river total length is 37 km. It rises on the slopes of Monte Cervati (1899 m) and about 15 km downstream, after the contribution of some secondary branches, the river is intercepted by an artificial dam called "Sabetta", whose water storage is utilized for hydropower production. About 2 km downstream of the Sabetta dam, near the village of Caselle in Pittari, the Bussento river sinks in a karst formation (a sinkhole) called "Inghiottitoio del Bussento" and resurfaces after 5 km of underground flow near the village of Morigerati. During the last part of its course Bussento meets, on the right side, its two greater affluents: the Sciarapotamo torrent and subsequently the Isca delle Lame torrent. The river flows in the Tyrrhenian sea, near the village of Policastro Bussentino.

Although the river is relatively short, it is characterized by two different conformations. In the upstream part the river shows mountain torrent characteristics: reaches with high slopes, rocky bed and an embedded water. Instead, in the part between the sinkhole and the sea, slopes are gentle and the gravel bed and is mostly embanked.

4.2 Utilized hydrologic data

Rainfall, discharges and temperature data, for the time period between 1954 and 1968, have been recorded by "Servizio Idrografico" of " Ministero dei Lavori Pubblici", and spreaded through the "Annali Idrologici" (Napoli). In this study have been utilized rainfall data of all the stations referred, in "Annali Idrologici" to the Bussento river.
Rainfall and temperature data, for the time period between 2002 and 2012, have been supplied by $http://www.scia.isprambiente.it/$.
Solar radiation data have been supplied by the site: $http://clisun.casaccia.enea.it/$.
A summary of the available data is presented in Tables 4.1, 4.2, 4.4, 4.3, 4.5 and 4.6.
The spatial position of the stations and the morphology of the catchment are reported in Figure 4.1.

Period	Station	Kind of measure
1954-1968	Caselle in Pittari	Daily averaged discharge $[m^3/s]$

Table 4.1: Utilized discharge data

Period	Station	Kind of measure
1954-1963	Sanza, Morigerati, Casaletto Spartano	Daily rainfall depth $[mm]$
1964-1968	Sanza, Morigerati, Casaletto Spartano, Caselle in Pittari	Daily rainfall depth $[mm]$
2002-2012	Sanza	Daily rainfall depth $[mm]$

Table 4.2: Utilized rainfall data

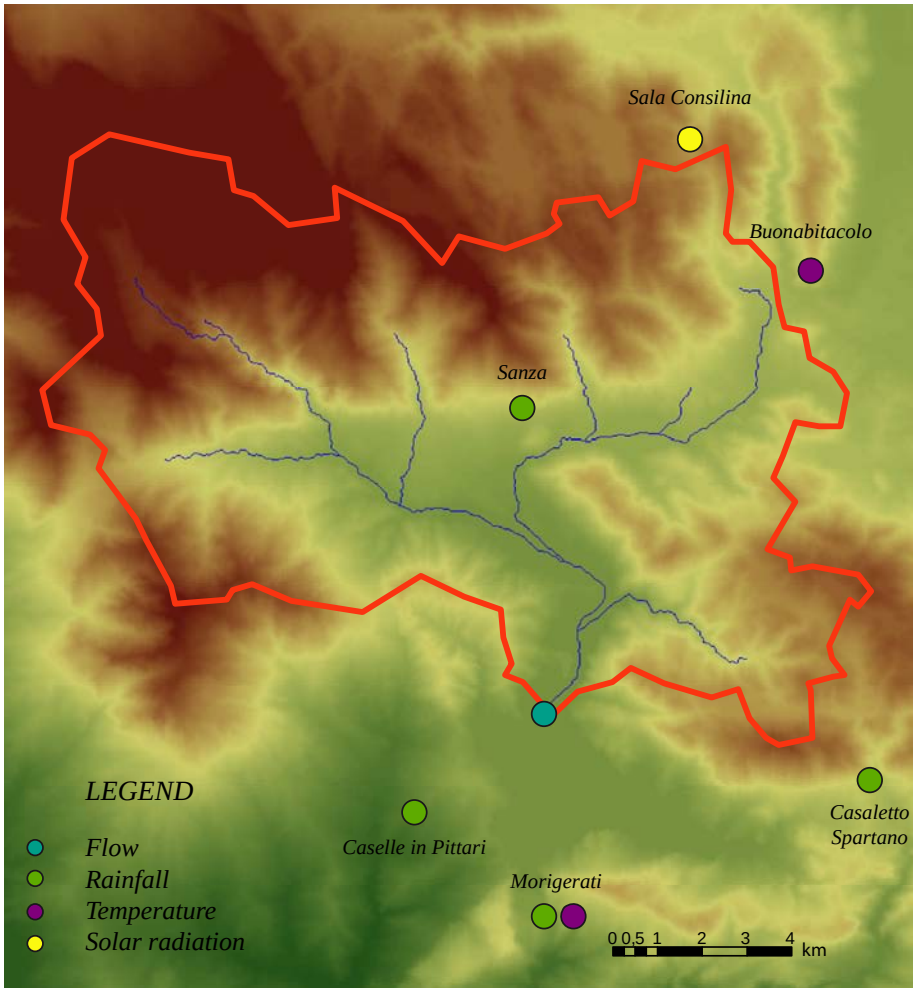

Figure 4.1: Morphology of the catchment and indicative spatial position of the measure stations.

Period	Station	Kind of measure
1994-1999	Sala Consilina	Monthly averaged solar radiation $[\frac{Mj}{m^2 d}]$

Table 4.3: Utilized solar radiation data

Period	Station	Kind of measure
1954-1968	Morigerati	Monthly averaged daily minimum and maximum temperatures [$^{\circ}C$]
1999-2012	Buonabitacolo	Monthly averaged daily minimum and maximum temperatures [$^{\circ}C$]

Table 4.4: Utilized temperature data

Period	Station	Kind of measure
1999-2012	Buonabitacolo	Daily mean wind velocity $[m/s]$
1999-2012	Buonabitacolo	Daily minimum and maximum relative umidity [%]

Table 4.5: Utilized wind speed and relative humidity data

Period	Type of vegetation	Kind of measure
$k_C(t)$	Conifere mediterranee	Monthly crop coefficient
	Boschi di leccio	Monthly crop coefficient
	Boschi di faggio	Monthly crop coefficient
	Pascolo	Monthly crop coefficient
	Sclerofille	Monthly crop coefficient
	Gariga	Monthly crop coefficient

Table 4.6: Utilized $k_C(t)$

Chapter 5

Evaluation of the hydrologic regime and hydropower potential of the Bussento river

The hydrologic model proposed in chapter 2 is applied to the Bussento river at Caselle in Pittari, a catchment of about 113 km^2. The aim is to obtain a complete and consistent characterization of the hydrologic regime of the river through the probability density function of the discharges, to be used for the evaluation of the hydropower potential of the river.

The procedure to obtain the PDF parameters, defining the streamflow distribution, is divided into two step.

- A first model is carried out using discharge and rainfall data available for the period 1954-1968, where data are sufficient for the application of the method accordig to the procedures described in section 2.4. This will allow a better understanding of the hydrologic regime and to check the validity of the modelization.
- Thus, the model will be applied to the time period 2002-2012. In this period there is a lack of discharge data so it is necessary to take as a reference the informations previously gained on the hydrologic regime.

5.1 Application of the model to the time period 1954-1968

5.1.1 Manipulation of data and definition of the seasons

In this part of the study these data are used:

- Discharge: data from Table (4.1) of period 1954-1968;
- Rainfall: data from Table (4.2) of period 1954-1968;
- Temperature: data from Table (4.4) of period 1954-1968;
- Solar radiation: data from Table (4.3) of period 1999-2012;
- Wind speed and relative humidity: data from Table (4.5) of period 1999-2012;

Daily rainfall data, given in $[mm]$ have been averaged between the stations and have been transformed in $[cm]$. So the mean value of the daily rainfall of the day i in $[cm]$, being n the number of stations, is:

$$\overline{h_i} = \frac{\sum_{j=1}^{n} h_{i,j}}{10n} \tag{5.1}$$

where $h_{i,j}$ is the measure of the daily rainfall made by station j for the day i in $[mm]$.

Concerning discharge data, which were expressed in $[m^3/s]$, discharges have been transformed into specific discharges, following the relation:

$$Q[cm/d] = Q[m^3/s]\frac{86400}{Area10^4} \tag{5.2}$$

where $Area$ is the area of the catchment.

The seasonal subdivision of data for this catchment has been done considering three different seasons:

- **Season 1** (november, december and january); this season has been called **"recharge" season**, due to the fact that it shows abundant rainfall precipitation and relevant flow peaks but a low runoff coefficient ($C_R \cong 0.6$), as a significant part of the rainfall is stored.
- **Season 2** (february, march and april); this season has been called **"wet" season** because of the significant precipitation and the high runoff coefficient.

Parameter	"Recharge"	"Wet"	"Dry"
Mean frequency $\lambda_P\,[d^{-1}]$	0.60	0.52	0.36
Mean water depth $\alpha_P\,[cm]$	1.29	0.95	0.67

Table 5.1: Rainfall parameters of period 1954-1968

This season shows relevant flow peaks and persistent flows. Owing to a significant contribution of the baseflow, in this season runoff coefficients are larger than 1.

- **Season 3** (may, june, july, august, september and october); this season has been called **"dry" season** because of the scarce rainfall precipitation and low discharges. In this season there are just a few flow peaks, in response to the major rainfall events. Notwithstanding the reduced precipitation, during this season the observed discharge is always positive, suggesting the presence of a baseflow due to carryover among the seasons. In this season, typical values of the runoff coefficient are larger than 1.

The value of seasonal λ_P (mean frequency of rainfall events $[d^{-1}]$) and α_P (mean rainfall depth in wet days $[cm]$) can be obtained for each season. The mean precipitation $\langle P \rangle$ is:

$$\langle P \rangle = \lambda_P \alpha_P \tag{5.3}$$

The parameters λ_P and α_P for the three seasons are reported in Table 5.1.
Discharge data have been subdivided according to the seasons previously identified and the mean specific flow $\langle Q \rangle$ was then calculated.
The mean frequency of streamflow generating rainfall events, λ, was calculated using the equation (2.12), providing the results shown in Table 5.2.

5.1.2 Hypodermic discharge PDF parameter estimation

The mean specific seasonal discharge $\langle Q \rangle$ has been separated into $\langle Q_H \rangle$ and $\langle Q_B \rangle$, according to equation (2.17).
All the parameters defining the PDF of the hypodermic flow are calculated following the procedure explained in chapter 2.5.1.

Parameter	"Recharge"	"Wet"	"Dry"
Mean frequency $\lambda\,[d^{-1}]$	0.36	0.58	0.40
Mean frequency $\lambda_P\,[d^{-1}]$	0.60	0.52	0.36

Table 5.2: Comparison between mean frequency of flow generating rainfall events and mean frequency rainfall events of period 1954-1968

Parameter	"Recharge"	"Wet"	"Dry"
Mean frequency $\lambda_H\,[d^{-1}]$	0.17	0.14	0.04
Mean water depth $\alpha_P\,[cm]$	1.29	0.95	0.67

Table 5.3: Hypodermic flow parameters for period 1954-1968

In particular λ_H is calculated using the equation (2.38), and then the value of $\langle Q_H \rangle$ is obtained with equation (2.23) and $\langle Q_B \rangle$ with (2.39). Mean specific baseflow and hypodermic discharges are reported in Table 5.7. Parameters defining $\langle Q_H \rangle$ are reported in Table 5.3.
The recession time constant k is calculated using total discharge values of the time period 1954-1968 and equation (2.40) suitably modified.
Parameters defining $p_H(Q_H)$ for the time period 1954-1968 are reported in Table 5.4.

5.1.3 Hydrologic regime characterization

Some assumptions have been made in order to characterize the seasonal baseflow, based on the observed rainfall, baseflow and mean discharges:

- in the "recharge" season, baseflow is mainly due to slow runoff of rainfall

Parameter	"Recharge"	"Wet"	"Dry"
Shape parameter $\lambda_H/k\,[-]$	0.65	0.64	0.28
Rate parameter $\alpha_P k\,[cm/d]$	0.34	0.21	0.07

Table 5.4: Hypodermic PDF parameters for period 1954-1968

precipitated during the recharge season itself, because of the shortage of rainfall precipitation in the previous period. For this reason, "recharge" has to be seen as the beginning of the hydrologic year. Probably a fraction of the water stored will contribute to the runoff of the following seasons.

- in the "wet" season, baseflow assume the highest value, due to the contributions of carryover from the previous season and slow flows related to precipitation. A fraction of the precipitation occurring during this season will contribute to the baseflow of the "dry" season.
- in the "dry" season, the baseflow is due to the contributions of slow subsurface flow mainly originated during the previous season. In fact it is typically very low and will be neglected.

These observations gives also some indications about the correlations between seasonal rainfall and baseflow, which are necessary for the calculation of the variance of the baseflow.

Evapotranspiration parameters are calculated referring to temperature data and to the other climate data in section 4.2.

Seasonal potential evapotranspiration is calculated for seasons "recharge" and "wet" using Penman-Monteith equation, with 1954-1968 temperature data from Table (4.4), solar radiation data from Table (4.3) and wind speed and relative humidity from Table (4.5).

Crop coefficients in these seasons was been calculated averaging over the season itself crop coefficients of the most common plant species in the catchment, reported in Table (4.6).

Water stress coefficient, given the abundance and the frequency of the rainfall and the values of the temperatures, in these seasons is assumed to be unitary.

Parameters used for the calculation of $\langle ET \rangle$ of seasons "Recharge" and "Wet" are reported in Table (5.5).

Instead, the evapotranspiration for the season "dry" is obtained in a different way, under some assumptions. In this season, rainfall events generating flow are extremely rare as can be seen from the value $\langle Q_H \rangle_D$ (Table (5.7)). This suggest that rainfall pulses are almost totally filtered by the root zone. So for the "dry" season equation (2.22) is modified into:

Parameter	"Recharge"	"Wet"	"Dry"
Crop coefficient $k_C(t)$	0.47	0.53	-
Water stress coefficient $k_S(s)$	1	1	-
Potential evapotranspiration $\langle ET_0 \rangle$	0.20	0.35	-

Table 5.5: Parameters for "Recharge" and "Wet" $\langle ET \rangle$ estimation for period 1954-1968

Parameter	"Recharge"	"Wet"	"Dry"
Mean frequency $\lambda_S\,[d^{-1}]$	0.35	0.18	0
Mean water depth $\alpha_P\,[cm]$	1.29	0.95	0.67

Table 5.6: $\langle Q_S \rangle$ parameters for period 1954-1968

$$\langle ET \rangle_D = \langle P \rangle_D - \langle Q_H \rangle_D \tag{5.4}$$

having assumed $\langle Q_S \rangle_D$ assumed to be null. The resulting values of seasonal evapotranspiration are reported in Table 5.7.

Once found the value of $\langle ET \rangle$, it is possible to find out the values of $\langle Q_S \rangle$ for the "recharge" and the "wet" season using equation (2.22), whose parameters are reported in Table 5.6:

Henceforth, the values of $\langle Q_{Bout} \rangle$, the baseflow fraction originated outside of the basin, are obtained using equation (2.35).

$\langle Q_{Bin} \rangle_i$, the fraction of baseflow coming from the catchment itself, is calculated with equation (2.16), and consequently values of carryover discharges can be calculated using equation (5.5):

$$\langle Q_{Bin} \rangle_i = \left(\langle Q_{Bco} \rangle_{i-1} + \langle Q_S \rangle_i \right) - \langle Q_{Bco} \rangle_i \tag{5.5}$$

Concerning the seasonal carryover the following assumptions are done:

- the "recharge" season does not receive carryover from the dry season, but it only contributes to the discharge of the wet season. Thus, equation (5.5) becomes:

Parameter	"Recharge"	"Wet"	"Dry"
$\langle P \rangle$ $[cm/d]$	0.77	0.49	0.24
$\langle ET \rangle$ $[cm/d]$	0.10	0.20	0.22
$\langle Q_H \rangle$ $[cm/d]$	0.22	0.13	0.03
$\langle Q_S \rangle$ $[cm/d]$	0.46	0.17	0.00
$\langle Q_{Bco} \rangle$ $[cm/d]$	0.31	0.14	0.00
$\langle Q_{Bin} \rangle$ $[cm/d]$	0.15	0.34	0.14
$\langle Q_{Bout} \rangle$ $[cm/d]$	0.1	0.1	0.10
$\langle Q_B \rangle$ $[cm/d]$	0.25	0.44	0.24
$\langle Q \rangle$ $[cm/d]$	0.47	0.56	0.27

Table 5.7: Mean specific discharges for period 1954-1968

$$\langle Q_{Bco} \rangle_R = \langle Q_S \rangle_R - \langle Q_{Bin} \rangle_R \tag{5.6}$$

- the "wet" season receives carryover from the previous season, and also contributes to the dry season. Thus, equation (5.5) becomes:

$$\langle Q_{Bco} \rangle_W = (\langle Q_{Bco} \rangle_R + \langle Q_S \rangle_W) - \langle Q_{Bin} \rangle_D \tag{5.7}$$

- the "dry" season receives carryover discharge from the wet season, but it does not contributes to the streamflows in the recharge season. This is because during dry season all slow baseflow is assumed to run out. Being also:

$$\langle Q_{Bco} \rangle_D = 0 \tag{5.8}$$

  Equation (5.5) becomes:

$$\langle Q_{Bco} \rangle_W = \langle Q_{Bin} \rangle_D \tag{5.9}$$

The major quantities defining the hydrologic regime in period 1954-1968 are summarized in Table 5.7:

5.1.4 Baseflow discharge PDF parameter estimation

The estimation of the parameters concerning the baseflow PDF has been carried out following the procedure described in chapter 2.5.2.
For each season correlations between $\langle Q_B \rangle$ and $\langle P \rangle$ have been identified, as described below:

- "recharge" season: it is assumed that $\langle Q_B \rangle$ correlates with the excess rainfall, defined as the difference between $\langle P \rangle$ and the storage capacity $nZr(s_1 - s_W)$, where: n is the porosity of the soil, Zr the root zone depth, s_1 the minimum soil moisture for runoff and s_W the wilting point. The term $nZr(s_1 - s_W)$ represents the water gap that rainfall has to fill at the beginning of the "recharge" season, in order to trigger runoff.
  Hence, the coefficient of variation of $\langle Q_B \rangle$ in the recharge season is calculated as:

$$CV(\langle Q_B \rangle_R) = CV(\langle P \rangle_R - (nZr(s_1 - s_W))) \tag{5.10}$$

- "wet" season: as a carryover contribution comes from the recharge season, the baseflow is correlated to the rainfall observed during both the wet and recharge seasons. Recharge and wet season rates are thus weighted with two coefficients, respectively θ_R and θ_W, that are calculated as:

$$\theta_R = \frac{\langle Q_{Bco} \rangle_R}{\langle Q_{Bco} \rangle_R + \langle Q_S \rangle_W} = 0.64 \tag{5.11}$$

$$\theta_W = \frac{\langle Q_S \rangle_W}{\langle Q_{Bco} \rangle_R + \langle Q_S \rangle_W} = 0.36 \tag{5.12}$$

  Thus:

$$CV(\langle Q_B \rangle_W) = CV(0.64 \langle P \rangle_R + 0.36 \langle P \rangle_W) \tag{5.13}$$

- "dry" season: a carryover contribution comes from the previous season, so the baseflow in dry season is correlated to the observed precipitation during wet and recharge seasons. The weights associated to these contributions are the same as in equation (**??**)

Parameter	"Recharge"	"Wet"	"Dry"
Shape parameter $\frac{\langle Q_B \rangle^2}{var(\langle Q_B \rangle_i)}$ $[-]$	8.80	19.36	18.58
Rate parameter $\frac{var(\langle Q_B \rangle_i)}{\langle Q_B \rangle}$ $[cm/d]$	0.03	0.02	0.01

Table 5.8: Baseflow PDF parameters for period 1954-1968

$$CV(\langle Q_B \rangle_D) = CV(0.64 \langle P \rangle_R + 0.36 \langle P \rangle_W) \tag{5.14}$$

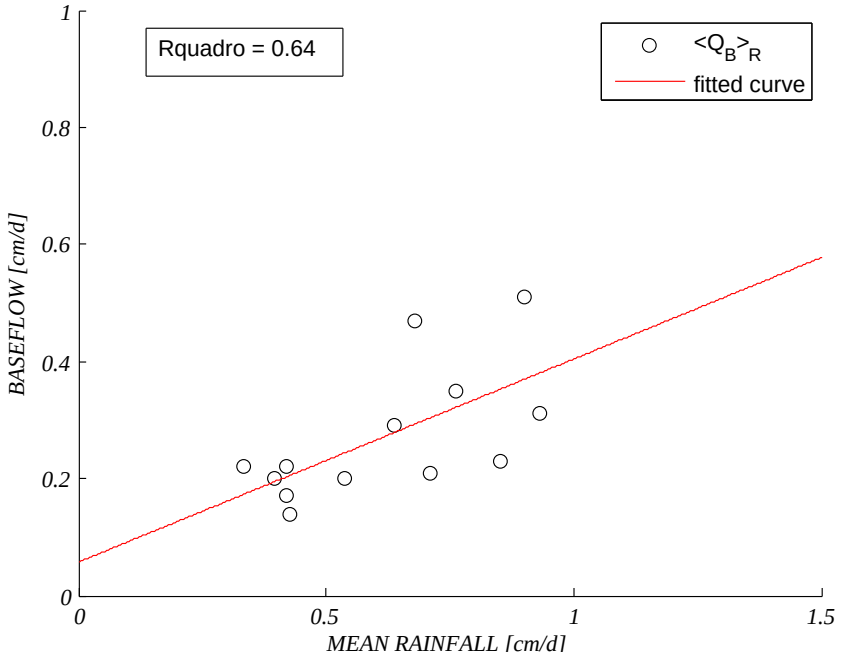

Figure 5.1: Recharge season: correlation between $\langle Q_B \rangle_R$ and $\langle P \rangle_R$

The correlation between $\langle Q_B \rangle$ and $\langle P \rangle$ is shown in Figures 5.1, 5.2 and 5.3, for the three different seasons. Relying on these relations variance of the baseflow has been calculated using equation (2.45). The parameters defining $p_B(Q_B)$ for the time period 1954-1968 are reported in Table 5.8.

5.1.5 Probability distribution of the overall discharge

Once $p_H(Q_H)$ and $p_B(Q_B)$ are defined for each season, total specific seasonal discharge PDF can be calculated from the convolution of these, using equation (2.36).

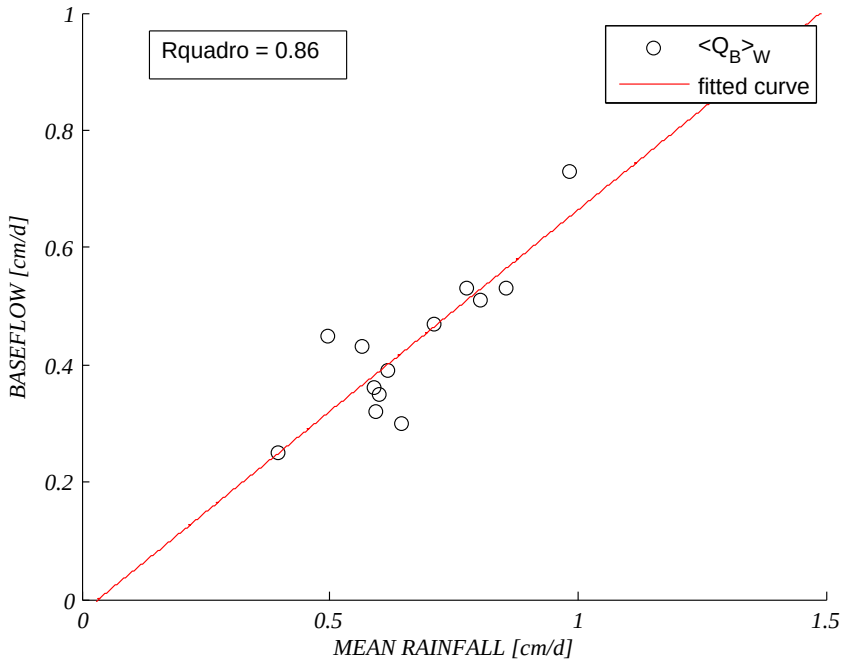

Figure 5.2: Wet season: correlation between $\langle Q_B \rangle_W$ and $(0.64\langle P \rangle_R + 0.36\langle P \rangle_W)$

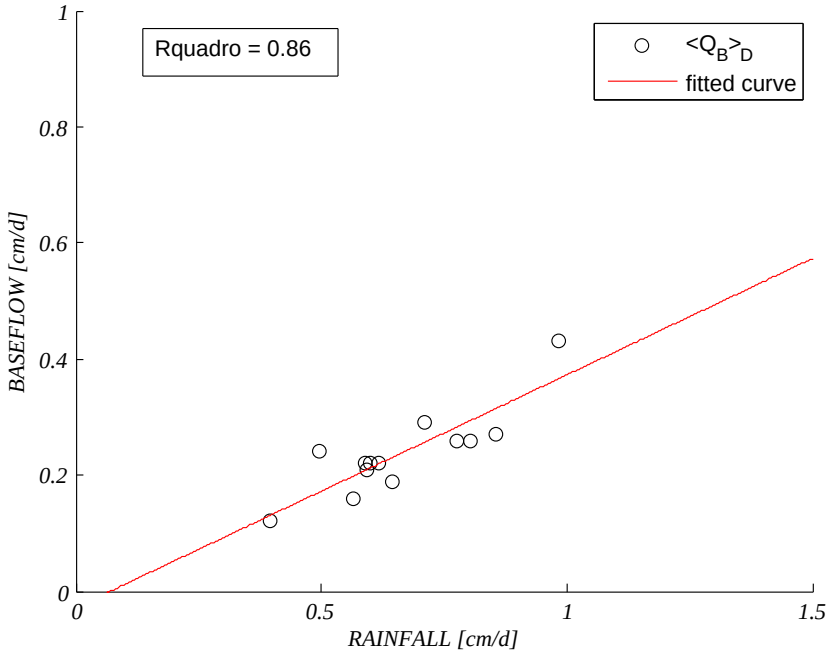

Figure 5.3: Dry season: correlation between $\langle Q_B \rangle_D$ and $(0.64\langle P \rangle_R + 0.36\langle P \rangle_W)$

Therefore, averaging the PDF of the three seasons, the PDF which represent the annual dynamic of the streamflow can be obtained.
In Figure 5.4 are reported annual discharges PDF and the observed discharge PDF.

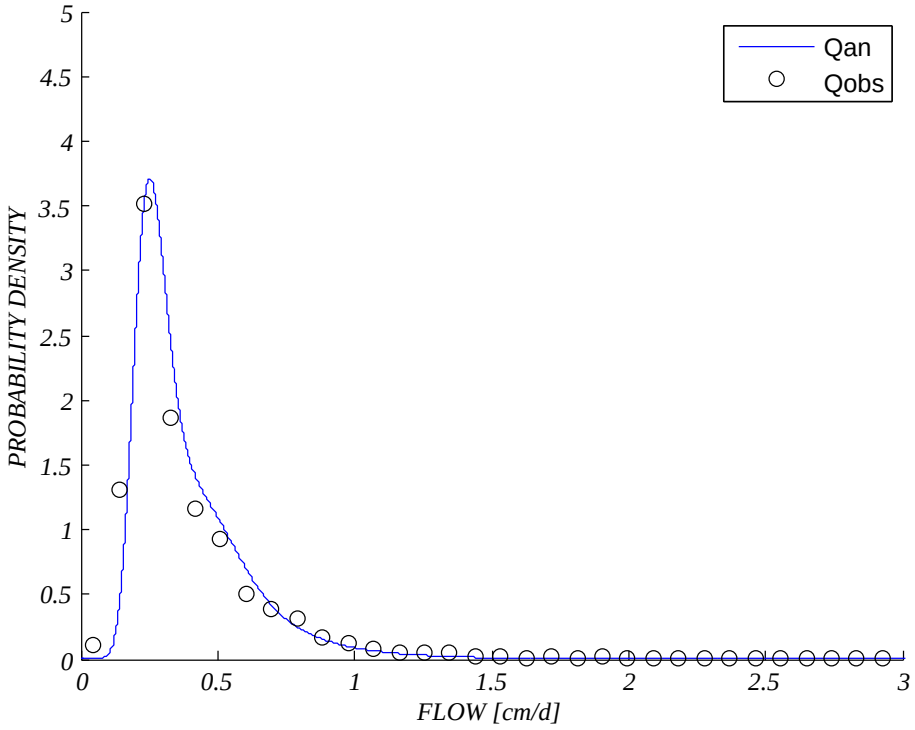

Figure 5.4: Probability density functions of the specific discharge (1954-1968). Comparison between the analytic PDF and the PDF obtained from observed data.

Observed discharges' PDF is well fitted by that obtained from the hydrological model. The model actually represent the hydrologic regime of the catchment, so it can be applied successfully to time period 2002-2012.

5.2 Application of the model to the time period 2002-2012

5.2.1 Elaboration of data and seasonal subdivision

In this part of the study these data are used:

- Rainfall: data from Table (4.2) of period 2002-2012;

- Temperature: data from Table (4.4) of period 1999-2012;
- Solar radiation: data from Table (4.3) of period 1994-1999;
- Wind speed and relative humidity: data from Table (4.5) of period 1999-2012;

Seasons of reference are the same as those chosen for the hydrologic analysis of years 1954-1968.

Obtained rainfall parameters for period 2002-2012 are reported in Table 5.9.

Parameter	"Recharge"	"Wet"	"Dry"
Mean frequency $\lambda_P\,[d^{-1}]$	0.51	0.47	0.29
Mean water depth $\alpha_P\,[cm]$	1.38	1.13	0.98

Table 5.9: Rainfall parameters of period 2002-2012

5.2.2 Hypodermic discharge PDF parameter estimation

In this case the calculation of the shape and rate parameter for the seasonal $p_H(Q_H)$ presents some difficulties. The lack of dicharge data doesn't permit the direct calculation of parameter λ_H using equation (2.38), and consequently of $\langle Q_B \rangle$ using (2.39).

However it is possible to obtain the value of λ^* from equation (5.15):

$$\lambda^* = \frac{\langle P \rangle - \langle ET \rangle}{\alpha_P} \tag{5.15}$$

which is based only on evapotranspiration and rainfall information. These are available for the period 2002-2012, as detailed below:

- $\langle P \rangle$ can be calculated using (5.3) with parameters reported in Table (5.9).
- $\langle ET \rangle$ can be estimated in the same way explained in chapter 5.1.3, using $k_C(t)$ and $k_S(s)$ coefficients, defined therein calculating the potential evapotranspiration using the observed temperatures during the period 2002-2012 (Table (4.4)). Concerning "dry" season, the value of $k_S(s)$, wasn't specified (see chapter 5.1.3), has to be calculated using the equation:

Parameter	"Recharge"	"Wet"	"Dry"
Crop coefficient $k_C(t)$	0.47	0.53	0.66
Water stress coefficient $k_S(s)$	1	1	0.55
Potential evapotranspiration $\langle ET_0 \rangle$	0.18	0.33	0.58

Table 5.10: Parameters for "Recharge", "Wet" and "Dry" $\langle ET \rangle$ estimation for period 2002-2012

Parameter	"Recharge"	"Wet"	"Dry"
Mean frequency $\lambda_H\,[d^{-1}]$	0.14	0.13	0.08
Mean frequency $\lambda_S\,[d^{-1}]$	0.30	0.18	0
Mean water depth $\alpha_P\,[cm]$	1.38	1.13	0.98

Table 5.11: $\langle Q_H \rangle$ and $\langle Q_S \rangle$ parameters for period 2002-2012

$$k_S(s) = \frac{< ET >}{k_C(t) < ETo >} \tag{5.16}$$

where $\langle ET \rangle$ and $\langle ET_0 \rangle$ are referred to the period 1954-1968.

Parameters used for that calculation are reported in Table 5.10.

Once λ^* is obtained, assuming that the ratio:

$$\theta = \frac{\lambda_S}{\lambda^*} \tag{5.17}$$

calculated for the period 1954-1968 also applies to the period 2002-2012, the current parameters λ_H and λ_S can be easily determined as:

$$\lambda_H = (1 - \theta)\lambda^* \tag{5.18}$$

$$\lambda_S = \theta\lambda^* \tag{5.19}$$

Values of λ_H, λ_S and α_P are reported in Table 5.11.

Furthermore, it is assumed also that the value of the recession rate k is equal to that calculated for the period 1968-1954.

The parameters defining $p_H(Q_H)$ for the time period 2002-2012 are reported in Table 5.12.

Parameter	"Recharge"	"Wet"	"Dry"
Shape parameter $\lambda_H/k\,[-]$	0.53	0.59	0.57
Rate parameter $\alpha_P k\,[cm/d]$	0.36	0.25	0.15

Table 5.12: Hypodermic PDF parameters for period 2002-2012

5.2.3 Hydrologic regime characterization

Once values for the hypodermic flow are calculated, for a complete definition of the hydrologic regime it is necessary to define the baseflow discharge. Mean specific baseflow discharge is defined following equation (2.16).

$$\langle Q_B \rangle_i = \langle Q_{Bin} \rangle_i + \langle Q_{Bout} \rangle \tag{5.20}$$

Two main assumptions are made for the baseflow modeling in the 2002-2012 time period:

- the mean external contribution $\langle Q_{Bout} \rangle$ is assumed to be equal to that estimated in the time period 1954-1968.
- The other component of the seasonal baseflow, $\langle Q_{Bin} \rangle_i$, can be calculated starting from rainfall data. Correlations shown in Figures 5.1, 5.2 and 5.3 have been found between seasonal $\langle Q_B \rangle_i$ and a relative seasonal rainfall in the previously analyzed time period. Thus, being $\langle Q_{Bout} \rangle$ seasonally constant, $\langle Q_{Bin} \rangle_i$, can be calculated from:

  $$\langle Q_{Bin} \rangle_i = \langle Q_B \rangle_i - \langle Q_{Bout} \rangle \tag{5.21}$$

  where $\langle Q_B \rangle_i$ is obtained from the regression line in figures (5.1), (5.2) and (5.3).

Values of the seasonal mean specific total discharge $\langle Q \rangle$ are calculated using equation (2.17).

Seasonal carryover discharges are calculated in the same way as for 1954-1968 period, using equation (5.5). Accordingly the carryover mechanism between the seasons is assumed to be the same.

- "Recharge" season:

Parameter	"Recharge"	"Wet"	"Dry"
$\langle P \rangle$ $[cm/d]$	0.71	0.53	0.29
$\langle ET \rangle$ $[cm/d]$	0.09	0.18	0.21
$\langle Q_H \rangle$ $[cm/d]$	0.19	0.15	0.08
$\langle Q_S \rangle$ $[cm/d]$	0.41	0.20	0.00
$\langle Q_{Bco} \rangle$ $[cm/d]$	0.25	0.13	0.00
$\langle Q_{Bin} \rangle$ $[cm/d]$	0.16	0.32	0.13
$\langle Q_{Bout} \rangle$ $[cm/d]$	0.10	0.10	0.10
$\langle Q_B \rangle$ $[cm/d]$	0.25	0.42	0.23
$\langle Q \rangle$ $[cm/d]$	0.44	0.57	0.31

Table 5.13: Mean specific discharges for period 2002-2012

$$\langle Q_{Bco} \rangle_R = \langle Q_S \rangle_R - \langle Q_{Bin} \rangle_R \tag{5.22}$$

- "Wet" season:

$$\langle Q_{Bco} \rangle_W = (\langle Q_{Bco} \rangle_R + \langle Q_S \rangle_W) - \langle Q_{Bin} \rangle_D \tag{5.23}$$

- "Dry" season:

$$\langle Q_{Bco} \rangle_D = 0; \qquad \langle Q_{Bco} \rangle_W = \langle Q_{Bin} \rangle_D \tag{5.24}$$

Summarizing, all quantities defining the hydrologic regime in period 2002-2012 are in Table (5.13):

5.2.4 Baseflow discharge PDF parameter estimation

The estimation of the parameters concerning the baseflow PDF has been carried out following the same procedure previously outlined. Starting from the correlations between $\langle Q_B \rangle_i$ and $\langle P \rangle_i$, the variance of the baseflow has been calculated using equation (2.44). The parameters defining $p_B(Q_B)$ for the time period 2002-2012 are reported in Table 5.14.

Parameter	"Recharge"	"Wet"	"Dry"
Shape parameter $\frac{\langle Q_B \rangle^2}{var(\langle Q_B \rangle_i)}$ $[-]$	2.24	5.94	4.64
Rate parameter $\frac{var(\langle Q_B \rangle_i)}{\langle Q_B \rangle}$ $[cm/d]$	0.12	0.07	0.05

Table 5.14: Baseflow PDF parameters for period 2002-2012

5.2.5 Probability distribution of the overall discharge

Once $p_H(Q_H)$ and $p_B(Q_B)$ are defined for each season, total specific seasonal discharge PDF can be calculated from the convolution of these curves, using equation (2.36). Therefore, averaging the PDF of the three seasons, the PDF which represent the annual dynamic of the streamflow can be obtained.
In Figure 5.5 is shown the obtained PDF.

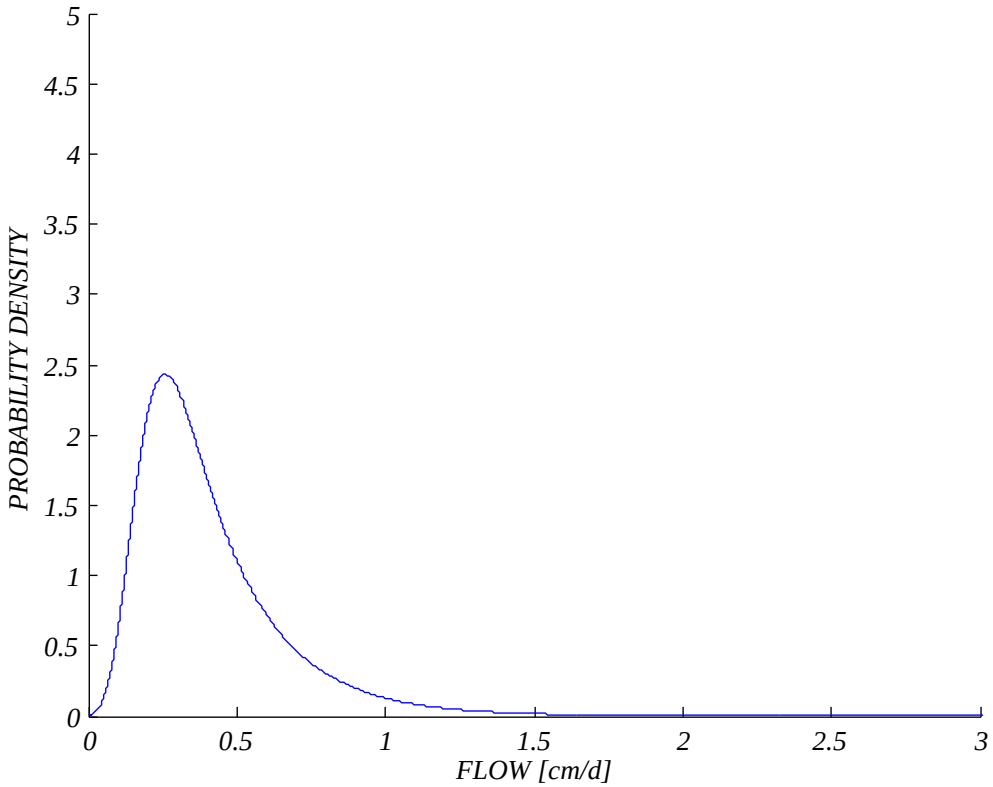

Figure 5.5: Annual probability density function of the specific discharge (2002-2012).

Figure 5.6 shows the estimated change in the hydrologic regime from 60s to the

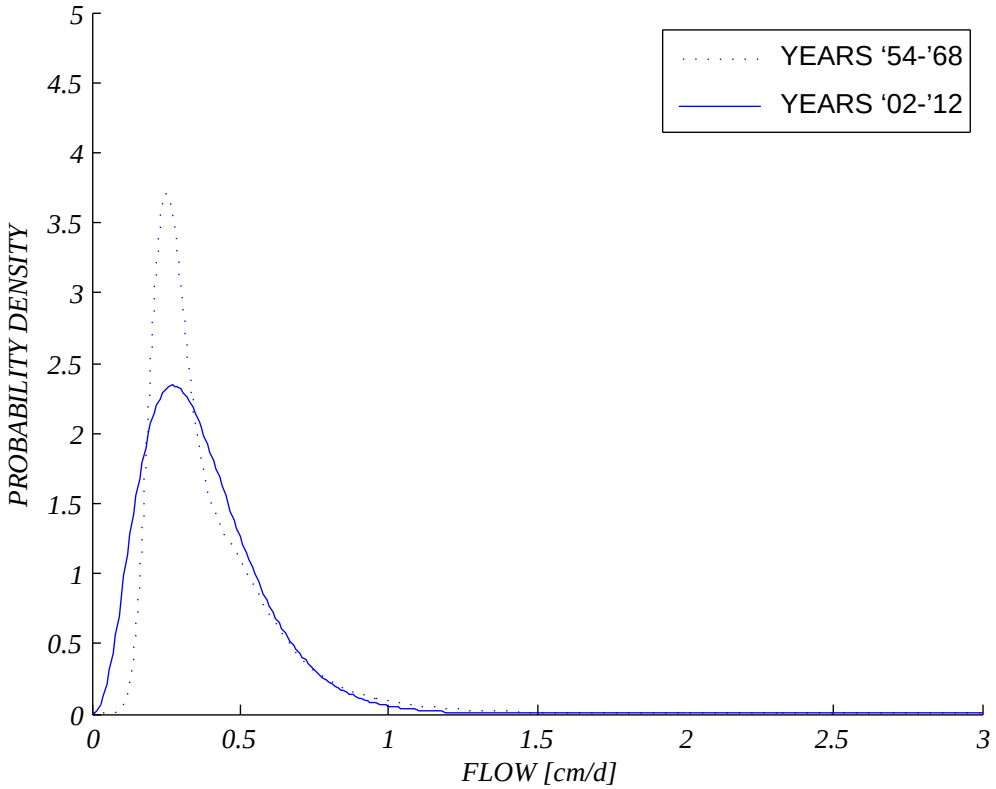

Figure 5.6: Probability density function of the specific discharge (reference time period 1954-1968 and 2002-2012).

last 10 years. The significant modifications shown in Figure 5.6 are certainly due to different climatic conditions. The baricenter of the PDF is not significantly shifted and its shape is less peaked. This means that the mean discharge remains the same, while the variance increases (cfr. Table 5.7 and Table 5.13). Being the mean evapotranspiration equal in both periods, this can be justified by rainfall, which mantains the same mean value in both periods, but increases its variability.

5.3 Estimate of the hydropower potential

The method discussed in chapter 3 has been applied to Bussento river, where the hydrologic analysis has provided a reliable estimate of the streamflows PDF at the closure section of Caselle in Pittari. This streamflow PDF constitutes the basis for the evaluation of the current hydropower potential of the river.

The approach to the evaluation of the hydropower potential of the catchment is based on the analysis of the catchment morphology. The morphology of the catchment has been evaluated using a DEM (Digital Elevation Model) of the terrain in the region where the catchment is located.
A specific software has been used to obtain informations like the stream network, the contributing area of different sub-catchments, the trend of elevations along the river bed.
In Figure 4.1 and 5.7 the morphology of the stream network is shown. This can be subdivided into three main branches contributing to the main stream, which has a very low slope (comprised between 0.0001 and 0.001). The search for a suitable site for a hydropower plant has been limited on these three branches, where the hydraulic jump is higher. Moreover, it is assumed that the lenght of the forced pipe (distance between the intake and the outflow) is about 1 km. This fact reduces drastically the exploitable contributing area, a decrease which is though compensated by the huge increase of the head (energy upstream minus energy downstream). The main consequence of this choice is that the hydrologic regime of the whole catchment, may be not representative of the regime observed in the reaches where the plant will be located.
The study has thus been carried on under the main hypothesis that the hydrologic regime identified for the catchment closed at Caselle in Pittari is representative for all the parts composing the whole basin.
The streamflow PDF in Figure 5.5, obtained from equation (2.36) as the convolution of $p_H(Q_H)$ and $p_B(Q_B)$ in period 2002-2012 has been first fitted with a gamma function to make easier the calculations. The PDF of specific discharges permits to estimate the streamflow PDF of an arbitrary sub-catchment with area A, by only modificating the rate parameter. Given the specific discharge Q $[cm/d]$, the discharge q $[m^3/s]$ which flows at the outlet of a catchment with area A $[km^2]$, can be approximated as:

$$q = f(A)\, Q \tag{5.25}$$

where $f(A) = \frac{A\, 10^4}{86400}$ is a conversion factor.
Using equation (2.46) and equation (2.47), the scale and rate parameters of the PDF of the streamflow PDF can be written as:

$$s_Q = \frac{\mu(Q)^2}{var(Q)} \tag{5.26}$$

$$r_Q = \frac{var(Q)}{\mu(Q)} \tag{5.27}$$

The change in units of measurements affects the mean μ and variance var of the discharge.

Therefore, the shape parameter s_q remains equal to s_Q, as can be seen in the following equation:

$$s_q = \frac{\mu(f(A)Q)^2}{var(f(A)Q)} = \frac{f(A)^2(\mu(Q)^2)}{f(A)^2(var(Q))} = \frac{\mu(Q)^2}{var(Q)} = s_Q \tag{5.28}$$

Instead, rate parameter r_q becomes:

$$r_q = \frac{var(f(A)Q)}{\mu(f(A)Q)} = \frac{f(A)^2 var(Q)}{f(A)\mu(Q)} = f(A)\frac{var(Q)}{\mu(Q)} = f(A)r_Q \tag{5.29}$$

The probability density function of the discharges q of a sub-catchment of area A can thus be written:

$$p(q) = \frac{(s_q)^{{r_q}^{-1}}}{\Gamma({r_q}^{-1})}\, q^{s_q - 1}\, e^{-q{r_q}^{-1}} \tag{5.30}$$

The hydropower potential analysis has been performed considering different intakes along the three branches of the network previously mentioned. For each one of these candidate intakes the values of q_{NPV} and NPV (Net Present Value) for $q_D = q_{NPV}$ have been calculated.

The application of the methods requires the preliminary determination of some parameters.

- **Cost parameters**: costs are assessed on the basis of equation (3.16).
  While the value of b, expressing the construction costs as a function of the capacity of the plant, is assumed to be constant, the parameter a depends on the constuction costs C and on the respective plant capacity q_D. Construction costs are not easily assessable, they can vary a lot from case to case because of the various locations, which for example can be easy or difficuilt to access, or require different kind of constructions and infrastructures. However, for the purpouse of this study, an averaged value of the parameter

Case study	Q_{PR} $[m^3/s]$	$C(Q_{PR})$ [M€]	a [M€/$\frac{m^3}{s}$]	$L[km]$
Valfredda Creek	0.15	1.00	3.121	1.3
Piova Creek	1.16	1.50	1.372	1.1
Ru Delle Rosse Creek	0.35	1.20	2.257	0.8

Table 5.15: Technical and economic characteristics of the three plants taken as reference. Q_{PR} is the project capacity, which affects the cost of the plant in measure given by the equation (3.16) and L is the impacted length of the river.

a would be sufficient, such estimate would allow to identify sites where an installation could be economically feasible.

Construction costs have been thus obtained from costs characteristics of three plants, situated in the Piave catchment in the province of Belluno, whose characteristics are reported in Table 5.15.

As can be seen in Table 5.15, the lenght of the forced pipes of these plants is similar ($L \approx 1km$). a is estimated by averaging the three values reported in Table 5.15.

- **MFD**: the Minimum Flow Discharge has been defined based on the currents prescriptions as the value of discharge that is exceeded with a probability of 96 %. From the point of view of the FDC, it is equivalent to find out the value of q that has a duration equal to 0.96. MFD has to be calculated for each closure section starting from equation (3.2), and using the correspondent streamflow probability density function.
- **Turbine type**: the type of turbine for each case is an important design feature because it determines the efficiency of the power plant. The choice has been made case to case, looking to the values of the hydraulic head: Pelton turbine have been used in case of large hydraulic heads ($> 100\ m$), Kaplan turbines have been used for the smallest hydraulic heads ($< 30\ m$), while Francis turbine in the other cases. All the plants are assumed to be equipped by a single turbine. Table 5.16 shows the parameters of the piecewise linear functions defining the efficiency curves of Francis turbines.

All the parameters required for the analytical optimization are now available. The procedure has been applied to 16 potential sites of installation in the three main

Parameters	Pelton	Francis	Kaplan
α_0	0.10	0.10	0.20
α_M	0.30	0.56	0.40
η_0	0.75	0.46	0.80
η_M	0.89	0.86	0.90

Table 5.16: Parameters defining the efficiency curves of different turbine types.

branches of the river, with an hydraulic head of 10 m at least. The calculation is done assuming constant renewable energy incentives during the next 15 years (energy price of 0.22 $€/kWh$).

5.3.1 Results

The results of the optimization procedure, expressed by equation (3.18), are graphically presented in Figure 5.7. In Table 5.17 are reported the obtained values.
Suitable sites for the intake have been localized along all the three considered branches of the Bussento river. The choice of the turbine type has been made case to case, as previously said. The major earnings are leaded by sites characterized by high hydraulic jump and large contributing area, in fact these sites are localized near the middle of each branch, where is achieved the better compromise between these quantities. From Figure 5.17 it can be seen that the highest earnings should come from plants situated along the branch A. This is because along that the river leads the highest slopes, and the contributing area is relatively high. It can be seen also that along a tract of the upstream part of the branch B the potential hydropower has not been evaluated: this is becouse here the river bed slope is too low, and plants with the fixed forced pipe lenght cannot have a sufficient hydraulic head. In four cases the obtained NPV value is negative: these sites are characterized by low hydraulic head and can not be exploited profitably (neither using Kaplan turbines), because revenues are lower than costs even if $q_D = q_{NPV}$. Maybe particular turbines, specifically projected for small hydraulic heads and limited flows (on average less than 1 m^3), are suitable for the exploitation of these sites.

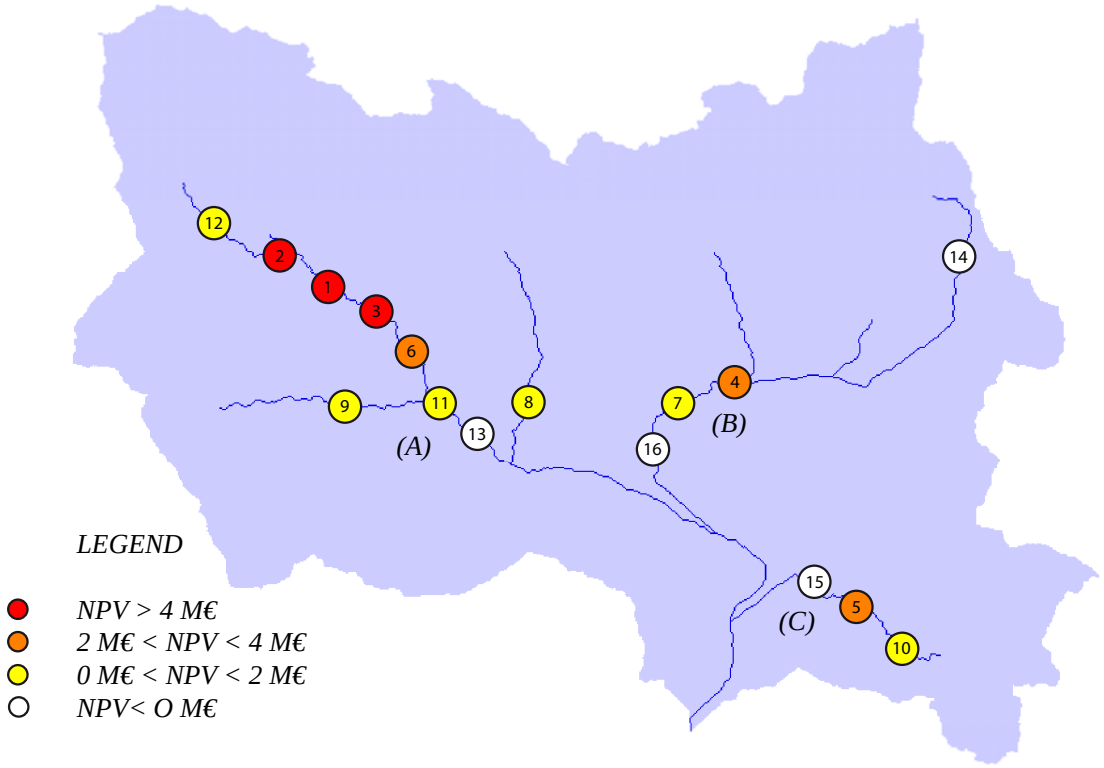

Figure 5.7: Evaluation of hydropower potential: positions of the considered sites.

Intake	A $[km^2]$	s_q [-]	r_q $\left[\frac{m^3}{s}\right]$	H $[m]$	Turbina [-]	MFD $\left[\frac{m^3}{s}\right]$	$\langle q \rangle$ $\left[\frac{m^3}{s}\right]$	q_{NPV} $\left[\frac{m^3}{s}\right]$	NPV [M€]
1	13.00	3.74	6.67	150	P	0.16	0.56	0.86	7.72
2	6,63	3.74	13,03	228	P	0,08	0,29	0,38	5.58
3	16.40	3.74	5.26	95	F	0.20	0.71	0.87	4.90
4	30.45	3.74	2.84	49	F	0.39	1.32	1.44	3.56
5	7.74	3.74	11.16	112	P	0.09	0.33	0.46	2.97
6	18.00	3.74	4.80	59	F	0.22	0.77	0.85	2.55
7	31.92	3.74	2.71	35	F	0.41	1.38	1.34	1.90
8	7.70	3.74	11.26	77	F	0.09	0.33	0.36	1.38
9	11.70	3.74	7.38	52	F	0.14	0.51	0.50	1.09
10	5,08	3.74	17,01	82	F	0,06	0,22	0,23	0.88
11	34.04	3.74	2.54	24	K	0.43	1.47	1.32	0.82
12	4,71	3.74	18,34	77	F	0,05	0,20	0,21	0.74
13	36.10	3.74	2.39	17	K	0.46	1.56	1.04	-0.08
14	5,05	3.74	17,11	30	K	0,06	0,22	0,09	-0.13
15	9.83	3.74	8.79	25	K	0.12	0.43	0.23	-0.15
16	32.22	3.74	2.68	15	K	0.41	1.39	0.65	-0.37

Table 5.17: Technical and economic characteristics of the evaluated sites.

Chapter 6

Conclusions

The aim of this work is the evaluation of the hydropower potential of the Bussento river. For this purpouse the hydrologic regime has been studied. To this aim, the probability density function of the streamflows has been modeled using a stochastic approach that explicitely includes informations about climate and landscape attributes.

The hydrologic regime has been modeled on the basis of two different data sets, one concerning the period 1954-1968 and one concerning the period 2002-2012. Because of the lack of discharge data in the period 2002-2012, the model is calibrated during the years 1954-1968, and then is applied to the period 2002-2012.

Using the obtained probability density function of the specific streamflows, an analysis of the hydropower potential of the Bussento river has been carried out. The evaluation evidenced a set of economically profitable sites for the plant intake, and the corresponding plant capacities.

The most significant results of this work are listed below.

- A preliminary analysis of the data sets has shown the complexity of the hydrologic regime of the Bussento river. The karstic territory in which the catchment is situated and the presence of external contributions lead to runoff coefficients that are very variable at monthly and annual timescales. In particular, runoff coefficients are, on average, <1 in cold and rainy months, and >1 in the rest of the year. The baseflow defined as the portion of the streamflow which has no causal relationship with flow generating rainfall events. Being the river discharges, in each season and in different measure, consti-

tuted by a fraction of baseflow, due to slow runoff, carryover and external contributions which cannot be directly quantified, only with an analysis of the flow regime and of the rainfall precipitation done on a longer timescale it is possible to understand and therefore describe the dynamic of the baseflow.

- The presence of baseflows significantly complicates the analytical description of streamflows dynamics and flow regimes. The complexity of the hydrologic regime leads to a necessary modification of the standard hydrologic model. The subdivision of the discharge into two different components permits a good representation of the hydrologic regime by means of physically meaningful quantities. In particular, the process of flow producing events has been splitted into two independent processes: the generation of hypodermic (fast) flow (with frequency λ_H), and the production of slow flow (with frequency λ_S). Slow runoff subtracts an amount of water to the root zone. Such water is released from the catchment as baseflow within longer timescales. These slow flows, jointly with the contribution of external sources, constitutes the baseflow of the Bussento river.

  Baseflow contributions to streamflows are well represented by a gamma distribution whose parameters have been calibrated based on the observed mean and variance of mean daily rainfall. Causal relationships between seasonal baseflow and precipitation have been identified through regression analysis. The method proposed for the modelization of the river flow regime in presence of baseflow well represents the hydrologic behavior of Bussento at Caselle in Pittari.

- From the preliminary analysis done in this study, the Bussento river at Caselle in Pittari basin is suitable for the installation of run-of-river power plants.

  In particular, 16 sites have been found to be suitable to host the plant intake. These are situated along the three small branches of the river, upstream of the main valley where the outlet of Caselle in Pittari is located. In these sites the relative contributing area is much smaller than the area of the entire catchment where the hydrologic regime is analiyzed. This leads to a significative uncertainty in the estimate of the flow PDF used to analyze the earnings from the energy selling.

The method has allowed a proper evaluation of the maximum hydro-potential of the considered catchment. Nevetheless, given the complexity of the hydrologic regime found for the whole basin, it is reasonable to think that each suitable sub-basin would deserve a more specific analysis of the hydrological regime. In particular, the external contributions and the baseflows could be highly heterogeneous in space, thereby, implying a pronounced heterogeneity of the flow regime along the stream network.

Bibliography

[1] Basso, S., G. Botter (2012), Streamflow variability and optimal capacity of run-of-river hydropower plants, *Water Resources Research*

[2] Bertacchi, P., G. Celentani, G. Marchetti (1990), Indagine sulle risorse idroelettriche minori nel mezzogiorno d'Italia, *Convegno nazionale sulle prospettive di sviluppo nel Mezzogiorno e condizioni di operativitï£¡ del settore.*

[3] Botter, G., S. Basso, I. Rodriguez-Iturbe, and A. Rinaldo (2013), Resilience of river flow regimes, *Proc. Natl. Acad. Sci. U.S.A.*

[4] Da Deppo, L., C. Datei, P. Salandin (2011) Sistemazione dei corsi d'acqua, *DiCEA, University of Padova*

[5] Lazzaro, G., S. Basso, M. Schirmer, and G. Botter (2013), Water management strategies for run-of-river power plants: Profitability ad hydrologic impact between the intake and the outflow, *Water Resources Research*

[6] Marani, M., Processi e modelli dell'idrometeorologia. Un'introduzione, *DiCEA, University of Padova*

[7] Consulted site: *http* : *//www.isprambiente.gov.it*

[8] Consulted site: *http* : *//sit.regione.campania.it*